CHARLES UNIVERSITY

FACULTY OF PHARMACY IN HRADEC KRÁLOVÉ

Department of Biochemical Sciences

&

UNIVERSITY OF PORTO

FACULTY OF PHARMACY

Department of Biological Sciences

In vitro effects of 3-hydroxytyrosol on renal hypoxia and inflammation

Diploma thesis

Supervisors: Asst. prof. PharmDr. Iva Boušová, Ph.D.

Prof. Alice Santos-Silva, Ph.D.

Maria João Valente, Ph.D.

Porto and Hradec Králové 2020 Terézia Kamasová

„Hereby I declare that this thesis is my original author‘s work. All literature and other sources, which I used for the elaboration of this thesis, are stated in the references and properly cited in the text. The thesis has not been used to obtain different or the same degree.“

„Prehlasujem, že táto práca je mojím pôvodným autorským dielom. Všetka literatúra a ďalšie zdroje, z ktorých som pri spracovaní práce čerpala, sú uvedené v zozname použitej literatúry a v práci sú náležite citované. Práca nebola využitá na získanie iného alebo rovnakého titulu.“

……

Abstract

Charles University

Faculty of Pharmacy in Hradec Králové

Department of Biochemical Sciences

University of Porto

Faculty of Pharmacy

Department of Biological Sciences

Candidate: Terézia Kamasová

Supervisor: Asst. prof. PharmDr. Iva Boušová, Ph.D.

Prof. Alice Santos-Silva

Maria João Valente, Ph.D.

Title of diploma thesis: ***In vitro*** **effects of 3-hydroxytyrosol on renal hypoxia and inflammation**

Chronic kidney disease (CKD) results from a group of heterogeneous disorders affecting the kidneys. The renal hypoxia and hypoxia-derived oxidative stress, renal fibrosis, and inflammation are highly prevailing conditions appearing in the diseased kidney, contributing to the progression of CKD. Phytochemicals are an essential part of contemporary therapeutic strategies for the treatment of various diseases. 3-Hydroxytyrosol (HT), a phenolic compound extracted from olives and olive-derived products (e.g. olive oil), is believed to carry a potent antioxidant, anti-inflammatory, antithrombotic, bactericidal and bacteriostatic activity. The aim of this work was to determine the preventive effect of HT in hypoxic renal cells and evaluate the effect of HT on hypoxia-related inflammation, fibrosis, and oxidative stress, in order to summarize the value of this phenolic compound as a promising novel remedy in the treatment of CKD. A cell line of human renal proximal tubular cells (HK-2) was selected to examine the effects of chemically induced hypoxia, hypoxia-derived inflammation, oxidative stress, renal fibrosis, and cell death, and the *in vitro* effect of HT under these conditions. Cobalt chloride was used to induce hypoxic conditions, and the adequate concentration to use for this purpose was determined through the MTT reduction assay (cell viability), flow cytometric analysis of intracellular oxygen levels, and expression analysis of hypoxia-related genes by qPCR. To evaluate the effect of HT on hypoxic HK-2 cells, reactive oxygen and nitrogen species production and glutathione levels were assessed as markers of oxidative stress. The effect of HT on the expression of hypoxia and related mediators was also determined by qPCR. The activation of autophagy was confirmed by the formation of acidic vesicular organelles observed under a fluorescence microscope and quantified by flow cytometry using the acridine orange dye. Though not significant, HT showed a slight preventive effect on hypoxia-induced cell death. Importantly, it showed a notable beneficial effect on oxidative stress, as well as on the expression of key genes involved in hypoxia (*GAPDH*), inflammation (*IL6*), and renal fibrosis (*TGFB1*). Together, the obtained results suggest that HT can act as a relevant therapeutic approach in the treatment of CKD in the future, though further studies on this matter are still required.

Abstrakt

Univerzita Karlova

Farmaceutická fakulta v Hradci Králové

Katedra biochemických vied

Univerzita Porto

Farmaceutická fakulta

Katedra biologických vied

Kandidát: Terézia Kamasová

Školitel: Doc. PharmDr. Iva Boušová, Ph.D.

Prof. Alice Santos-Silva

Maria João Valente, Ph.D.

Názov diplomovej práce: **Účinky 3-hydroxytyrosolu na renální hypoxii a zánět *in vitro***

Chronické zlyhanie obličiek je spôsobené heterogénnou skupinou ochorení postihujúcich obličky. Renálna hypoxia a hypoxiou-vyvolaný oxidatívny stres, renálna fibróza a zápal, sú veľmi častými sprievodnými javmi v postihnutej obličke, prispievajúcimi k zhoršovaniu chronického zlyhania obličiek. Látky rastlinného pôvodu sú neoddeliteľnou súčasťou modernej medicíny v terapií rôznych ochorení. 3-Hydroxytyrosol, fenolická zlúčenina získaná extrakciou z olív a olivových produktov ako napríklad olivový olej, je nositeľom silnej antioxidačnej, protizápalovej, antitrombotickej, baktericídnej a baktériostatickej aktivity. Cieľom tejto práce bolo stanoviť preventívny efekt 3-hydroxytyrosolu v renálnych bunkách a určiť jeho efekt na hypoxiou-vyvolaný zápal, oxidatívny stres a renálnu fibrózu a tak zhrnúť prínos tejto fenolickej zlúčeniny ako sľubného moderného terapeutického prístupu v liečbe chronického zlyhania obličiek. Na skúmanie efektu chemicky-indukovanej hypoxie a hypoxiou vyvolaného zápalu, oxidatívneho stresu, fibrózy a bunkovej smrti a na skúmanie *in vitro* efektu hydroxytyrosolu v týchto podmienkach bola použitá bunečná línia ľudských proximálnych tubulárnych buniek (HK-2). Ako induktor hypoxie bol použitý chlorid kobaltnatý. Jeho optimálna koncentrácia pre nasledujúce pokusy bola stanovená pomocou testu MTT, na zistenie životaschopnosti buniek v jeho prítomnosti, pomocou prietokovej cytometrie, na stanovenie spotreby kyslíka v bunkách a pomocou qPCR analýzy expresie s hypoxiou súvisiacich génov. Na zhodnotenie efektu 3-hydroxytyrosolu na hypoxiu v HK-2 bunkách boli ako ukazovatele oxidatívneho stresu zvolené produkcia kyslíkových a dusikových radikálov, a hodnota glutatiónu. Expresia génov súvisiacich s hypoxiou bola taktiež stanovená pomocou qPCR. Aktivácia procesu autofágie bola potvrdená pomocou tvorby kyslých vezikúl zafarbených akridínovou oranžovou pozorovaním pod fluorescenčným mikroskopom a kvantifikovaním prietokovou cytometriou. 3-Hydroxytyrosol vykazoval len nevýrazný preventívny efekt na hypoxiou-vyvolanú bunkovú smrť. Významný efekt mal 3-hydroxytyrosol na oxidatívny stres, ako aj na expresiu génov súvisiacich s hypoxiou (*GAPDH*), zápalom (*IL6*) a renálnou fibrózou (*TGFB1*). Zo získaných výsledkov vyplýva, že 3-hydroxytyrosol môže do budúcnosti predstavovať vhodný terapeutický prístup v liečbe chronického obličkového zlyhania, ďalšie štúdie sú však potrebné na potvrdenie tejto hypotézy.

Content

1. Introduction

The whole experimental part of this work was carried out in the Laboratory of Biochemistry, Department of Biological Sciences, Faculty of Pharmacy, University of Porto under the supervision of Professor Alice Santos-Silva and Maria João Valente, Ph.D. Their group is focused on studying chronic kidney disease (CKD), end-stage renal disease (ESRD) and various related clinical complications (e.g. anemia, hypoxia, inflammation).

CKD is a widely prevalent heterogeneous disease caused by the deterioration of the renal function. It can result from many different chronic conditions, e.g. diabetes mellitus, hypertension, renal obstruction. There are several pathological changes happening inside the diseased kidney, such as the development of renal hypoxia, inflammation, or fibrosis. Renal hypoxia has an undeniable impact on the progression of CKD as the hypoxic environment induces the expression of various inflammation-, fibrosis-, and cell death-related genes, as an adaptive response to hypoxia. These pathological changes, amongst the uncontrolled progression of CKD, can represent a major life threat. Proper and early identification, combined with the correct treatment can, therefore, prevent the development of ESRD, which requires renal replacement therapy. Searching for novel therapeutic strategies is, therefore, vital to prolong the life-expectancy and comfort of the CKD patients, as well as to prevent unwanted complications.

Plant-derived products and their use in the treatment of various diseases has been gaining popularity in recent years. Olive and olive oil-derived products are easily acquired and affordable and, therefore, pose as appropriate alternatives and/or complementary treatment to chemically synthesized drugs. 3-Hydroxytyrosol (HT), a phenolic compound and the key effect carrier substance in olive oil, is believed to carry a potent antioxidant, anti-inflammatory, bactericidal, bacteriostatic and antithrombotic activity. The aim of this work was to evaluate the effects of HT on renal hypoxia and hypoxia-induced oxidative stress, inflammation, and renal fibrosis in a cultured renal cell line, to mimic the diseased kidney, in order to determine the potential of HT in the prevention of CKD progression.

2. Theoretical part

2.1. The kidney: anatomy and function

The urinary system (also known as a renal tract) is responsible for the formation and release of urine. Kidneys, ureters, bladder, and urethra are basic parts of the human urinary system. The kidneys are a bean-shaped pair organ on each side of retroperitoneal space, placed bellow rib cage, between T12-L3 vertebrae, on either side of the human spine. The left kidney is typically positioned slightly more superiorly than the right one. Each kidney has a superior and inferior pole. The parenchyma of the kidney consists of the outer part called the renal cortex and inner part called the renal medulla. The human kidney is characterized by a multilobular structure with approximately 14 conically shaped lobes, with the renal capsule facing base and renal calyx oriented tip, also called renal papilla (Hallgrímsson et al. 2003). Each of these lobes connects with a minor calyx, and urine flows through a porous region from medulla into each calyx. Minor calyces merge into major calyces, which form the renal pelvis directly connected with ureters (Figure 1). The main role of ureters is to transfer the urine to the bladder. The adrenal glands lie superomedially to the superior pole of each kidney. Each kidney is covered with a renal capsule, and a layer of fat called perirenal fat. The cortex and medulla are composed of the functional structure units of the kidney, the nephrons. This structure is crucial in filtering blood in order to produce urine. There are approximately 1 million nephrons in each human kidney. The nephron is composed of renal corpuscle (Bowman´s capsule and glomerulus) and the renal tubule. The renal tubule consists of the proximal tubule, loop of Henle, the distal tubule including a convoluted and straight part, and the collecting duct (Figure 2) (Hallgrímsson et al. 2003).

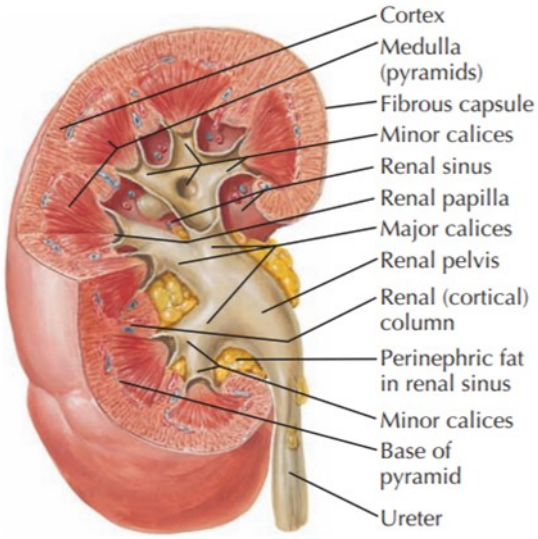

Figure 1 Sectioned right kidney (Netter 2012).

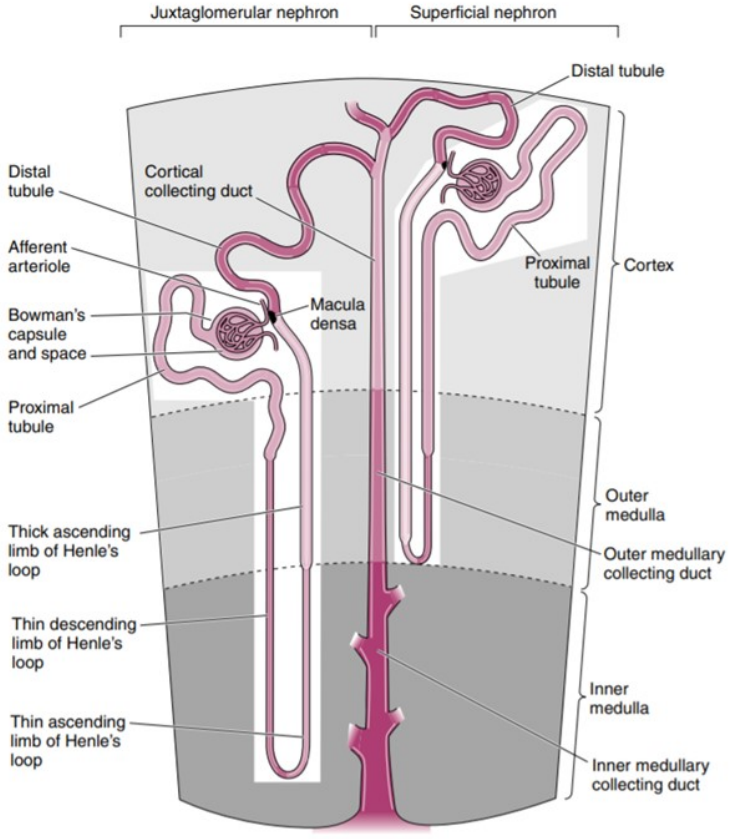

Figure 2 Juxtaglomerular (left) and superficial (right) nephron (Koeppen and Stanton 2013).

The main role of kidneys is to eliminate toxic metabolites, regulate blood homeostasis and blood pressure. The most significant physiological function of the kidney is the formation of urine and this process involves 3 crucial steps: (1) ultrafiltration of plasma by the glomerulus, (2) reabsorption of water and solutes from the ultrafiltrate, and (3) secretion of selected solutes into the tubular fluid. On average, 180 L of fluid is filtered by the glomeruli in every human a day, but only a small amount of filtered water and solutes are excreted into the urine. The most common solutes filtered, excreted and reabsorbed are Na^+, K^+, Ca^{2+}, HCO_3^-, Cl^-, glucose, and urea. The renal tubules regulate the volume and composition of urine by the process of reabsorption and secretion plus they control the precise volume, osmolality, pH, and composition of the intracellular and extracellular fluid compartments. Kidneys play another crucial role in the secretion of organic anions and cations, mainly by the proximal tubule, which contributes to the regulation of plasma levels of xenobiotics (e.g., antibiotics, diuretics, antineoplastics, statins, nonsteroidal anti-inflammatory drugs) or toxic compounds in general (Koeppen and Stanton 2013).

Angiotensin II, aldosterone, catecholamines, natriuretic peptides (atrial natriuretic peptide, brain natriuretic peptide), uroguanylin and guanylin are the most influential hormones regulating NaCl reabsorption and by that urinary NaCl excretion (Koeppen and Stanton 2013). Besides that, kidneys produce several hormones, important for vital functions of the human organism, which are involved in the blood pressure control, calcium metabolism, and erythropoiesis such as renin, calcitriol, and erythropoietin (Greene and Harris 2008).

2.2. Chronic kidney disease

Chronic kidney disease (CKD) may result from heterogeneous disorders affecting the function and structure of the kidneys. It is one of the worldwide public health problems with increasing incidence and prevalence in recent years. In the years 2007-2017, global absolute CKD prevalence increased by 28.2% among females and 25.4% among males (Fraser and Roderick 2019). It is believed that CKD belongs to key determinants of the poor health outcomes of several major non-communicable diseases (NCDs) such as diabetes, cancer, or cardiovascular disease (CVD) (Couser et al. 2011). The most common manifestations of

CKD include the progression of kidney failure, CVD, or complications connected to decreased kidney function (Levey et al. 2003). Along with CKD progression, the ability of the kidneys to clear the blood of waste products is slowly decreased. CKD can be defined as kidney failure when glomerular filtration rate (GFR) is lower than 60 mL/min/1.73 m^2 for 3 or more months, not depending on the cause. Another way to determine kidney damage can also be the presence of albuminuria, defined as an albumin-to-creatinine ratio greater than 30 mg/g in two of three spot urine specimens (Levey et al. 2005). As is shown in Table 1, CKD can be classified into five stages according to the GFR (Levey and Coresh 2012). CKD related clinical complications currently involve hypertension (resulting from NaCl and fluid retention, or possibly renin/angiotensin abnormalities), cardiovascular complications (dyslipidemia, heart failure, cardiomyopathy), anemia (marrow hypoplasia due to the reduced amount or absence of erythropoietin, iron deficiency-induced anemia), CKD induced mineral bone disorder (vitamin D deficiency-induced osteodystrophy), metabolic acidosis and electrolyte disorders as well as uremic symptoms (Greene and Harris 2008) (Bello et al. 2017).

Table 1 Classification of chronic kidney disease stages (Levey and Coresh 2012)

Stage	**GFR (mL/min/1.73m²)**
1	≥ 90
2	60–89
3	30–59
4	15–29
5	<15

By the location of impaired kidney function, CKD can be divided into three groups (1) pre-renal failure, (2) interstitial renal failure, and (3) post-renal failure (Greene and Harris 2008).

Pre-renal (1) failure is usually caused by factors that compromise renal perfusion. It begins as a reversible condition but can progress to established disease. The kidney relies on the blood supply of appropriate pressure to maintain glomerular filtration, therefore fluid

depletion, cardiac failure, or other shock states leading to hypovolemia and/or hypotension can be crucial in the development of pre-renal kidney failure. This is typical for an acute kidney injury (AKI), but it can also be an onset of CKD (Greene and Harris 2008).

Considering the excretory role of the kidney, which accumulates relatively high concentrations of the products of metabolism of various substances (e.g. xenobiotics), it is more prone to damage than other organs in the human body. Therefore, nephrotoxicity of both glomerular and tubular tissue is considered to be a common cause of (interstitial) (2) renal failure, which often leads to a chronic process (Greene and Harris 2008).

Post-renal (3) failure occurs as a consequence of urinary tract obstruction, often caused by stones, prostatitis, or tumor. It may be reversible depending on the cause of the obstruction but it can also lead to a chronic process (Greene and Harris 2008).

2.2.1. Pathophysiology of CKD

The main causes of CKD are diabetes mellitus and hypertension, obesity, cardiovascular disease, urethral obstruction and autoimmune and congenital diseases (Greene and Harris 2008), (Atkins 2005), (Levey and Coresh 2012). The three most common etiologies of CKD, i.e. diabetic nephropathy (DN), hypertensive nephropathy, and obstructive nephropathy, are described below.

2.2.1.1. Diabetic nephropathy

Diabetes mellitus is considered to be the major cause of the end-stage renal disease (ESRD), as much as a consequential cause of morbidity and increased mortality. Clinical manifestation of DN is connected to the pathological changes in all compartments of the kidney (Figure 3). The first clinical manifestations of DN are hyperfiltration and microalbuminuria. The thickening of the glomerular basement membrane, resulting from the build-up of extracellular matrix particles, is one of the earliest quantifiable changes. As the disease progresses, the further the deposition of matrix particles gets, which can result in the doubling of its usual size. Podocytes, glomerular endothelial cells, and mesangial cells are

also affected and might be a good predictor of diabetic nephropathy and its progression. In addition, hyperfiltration and hypertension cause biomechanical stress on these cells. Hyperglycemia and dyslipidemia also play a significant role in the progression of DN. It has been shown that hyperglycemia upregulates the expression of renin and angiotensin in mesangial cells, activating the renin–angiotensin–aldosterone (RAAS) pathway, contributing to the hyperplasia and hypertrophy of renal cells, as well as to albuminuria typical in DN. Inflammation and genetic influences play an important role in provoking and progressing of the DN (Atkins 2005).

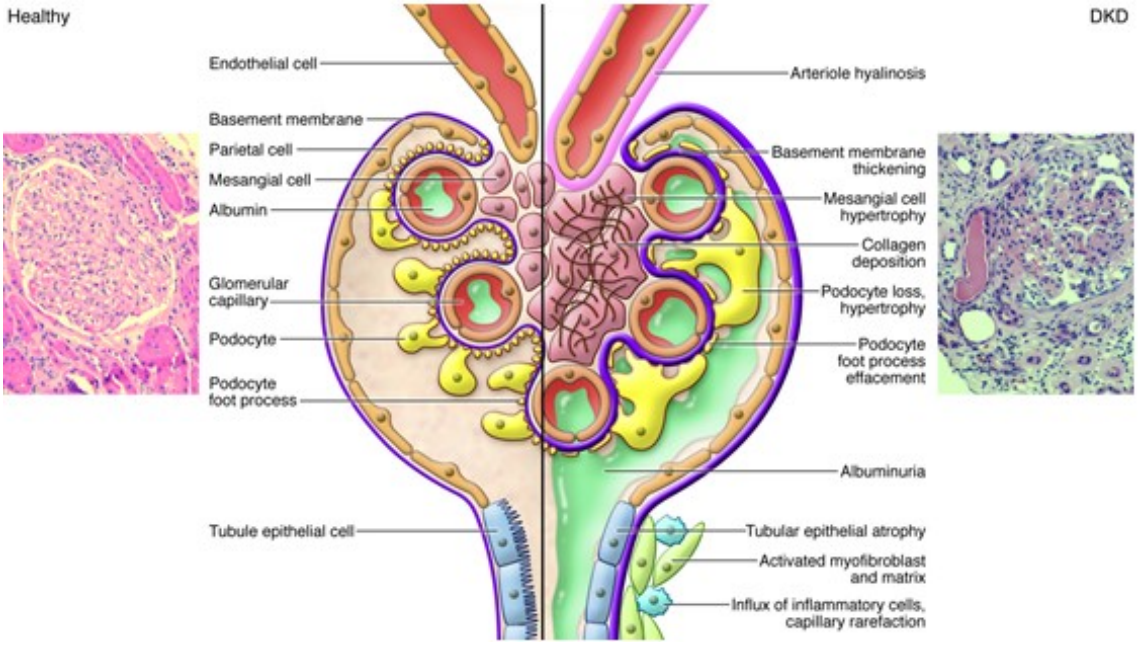

Figure 3: Normal kidney morphology (left) and structural changes in diabetes mellitus (right). Diabetic nephropathy induces structural changes, including the glomerular basement membrane thickening, loss of podocytes, and mesangial matrix expansion (Reidy et al. 2014).

2.2.1.2. Hypertensive nephropathy

In general, patients with more serious hypertension are more likely to develop CKD. Hypertensive nephropathy in CKD patients usually results from sodium and fluid retention, hormonal changes, activation of the sympathetic nervous system, or endothelial dysfunction.

Retention of sodium and volume expansion contributes to the development of hypertension the most. The ability to eliminate sodium and fluid decreases as kidney function disappears. Higher intake of sodium can also result in stiffening of the arteries, reduction in vascular nitric oxide (NO), promotion of inflammatory processes and it can lead to the lowering of renin activity, and angiotensin II production. Improper activation of RAAS has been involved in hypertension associated with CKD. Excess of angiotensin II is connected to a gradual loss of renal function, mainly through its stimulation of aldosterone release. Aldosterone contributes to increased blood pressure by the inhibition of NO. Volume expansion further potentiates the vasoactive effects of RAAS. Sympathetic nervous system also appears to be overactive in CKD, and it results in increased renin secretion and tubular sodium reabsorption (Townsend 2020).

2.2.1.3. Obstructive nephropathy

Obstructive nephropathy is a very common condition that occurs in all ages, usually resulting from the anatomic or functional lesions in the urinary tract. It is classified according to the degree, duration, and location of the obstruction. Obstruction can decrease GFR and renal blood flow, as well as cause tubular abnormalities such as reabsorption of water and solutes, inability to concentrate the urine, and damaged excretion of potassium and hydrogen. A common presentation of obstructive nephropathy is, for example, complete bilateral obstruction in AKI, partial but severe bilateral obstruction in CKD, and mechanical obstruction of the lower or upper urinary tract. It is known that obstructive nephropathy is closely associated with interstitial fibrosis, as a result of an imbalance between extracellular matrix protein synthesis and degradation (Klahr 2000).

2.2.2. Complications of CKD

There are several complications associated with CKD mainly anemia, inflammation, renal hypoxia, bone and mineral disease, and malnutrition (Levey et al. 2009).

2.2.2.1. Anemia

Anemia is a very common complication of CKD, which often develops early and progresses with the decline of renal functions. It contributes to decreased quality of life, increased rate of hospitalizations and comorbidities, further development of renal dysfunction, increased cardiovascular complications and mortality (Ribeiro et al. 2017). The main cause of anemia in CKD patients is the relative erythropoietin deficiency, which can be a result of decreased hormone production by the failing kidneys. Iron deficiency, inflammation, uremic toxins or chronic blood loss may also contribute to the development or worsening of the CKD anemia (Schrauben and Berns 2020).

Erythropoietin, as the main factor for controlling red blood cells (RBCs) production in the bone marrow, is a regulatory hormone, which stimulates RBCs maturation and their release into the circulation. In adults, erythropoietin is mainly produced by kidneys, whereas during fetal life, most of the erythropoietin is produced by the liver. It is a 165 amino acid glycoprotein, which contains carbohydrate chains with variable sialic acid content. There are various isoforms of erythropoietin in the circulation with different numbers of sialic acid parts, whose main function is to stabilize the molecule and they are also crucial for its biological activity. Regulation of the synthesis of erythropoietin is ensured primarily through the binding of the hypoxia-inducible factor (HIF). The erythropoietic system is responsible for maintaining the homeostasis of the RBCs supply, in order to reach sufficient oxygen delivery to the tissue (Schrauben and Berns 2020).

2.2.2.2. Renal hypoxia

Even though the kidney is one of the most oxygen perfused organs, considering its weight with the total received oxygen up to 80 mL/min x 100 g weight, oxygen pressure in the renal parenchyma is lower than in most other organs in the human body. Renal medulla can also be considered one of the parts in the human body with the lowest oxygen pressure. The reason being mostly the unique renal vasculature architecture. Branches of the renal arteries and veins, in both cortex and medulla, run in parallel and very closely for long distances. This allows the oxygen to diffuse from the arterial system into the venous system before it enters

the capillary bed (Eckardt et al. 2005). Most of the cardiac output directed to kidneys is mediated to the cortex in order to improve glomerular filtration and reabsorption of solutes. On the contrary, blood flow to the renal medulla is lower to preserve the osmotic gradients and optimize urinary concentration (Brezis and Rosen 1995). These limitations in renal tissue oxygen supply leave the kidney vulnerable to hypoxia, combined with lowered oxygen pressure, this combination plays an important role in the progression of CKD. According to Eckardt et al. (2005), there are three main points summarizing the impact of hypoxia and/or ischemia on the progression of CKD. Firstly, the peritubular capillary bed, which is considered to be the structural basis for acceptable oxygen delivery to tubular cells, is a very dynamic structure and CKD is often associated with a brisk decline in capillary density. This can be especially crucial, considering that there is a connection between GFR (as the main determinant of renal function) and peritubular oxygen supply. The peritubular capillaries structurally come from *vasa efferentia* of the glomeruli, so any interruption of glomerular blood flow (e.g. glomerular capillary obstruction, sclerosis) will weaken peritubular perfusion. Additionally, microvasculature dysfunction starts a hypoxic environment that provokes a fibrotic response in tubulointerstitial cells impacting previously unaffected capillaries, nephrons, and glomeruli, expanding the area of hypoxia and setting up the cycle of destruction to organ failure (Fine and Norman 2008). Secondly, tissue oxygen pressure usually declines in the affected kidney as a consequence of capillary loss and hypoperfusion. Thirdly, low oxygen pressure can also regulate cellular functions, and act as a stimulus for the induction of certain genes, e.g. oxygen-dependent gene regulation mediated by HIF (Eckardt et al. 2005).

HIFs are key regulators responsible for the induction of genes that mediate the adaptation and survival of cells in normoxic and hypoxic environments (Ke and Costa 2006). It is a family of heterodimeric transcription factors, consisting of oxygen-regulated HIF α-subunit and constitutively expressed β-subunit. Three α-subunits have been identified in mammals: HIF-1α, HIF-2α, HIF-3α. HIF-3α is the least well characterized of the three mentioned (Fine and Norman 2008). Each of these subunits is compiled of the carboxi-terminal transactivation domain (C-TAD) and amino-terminal transactivation domain (N-TAD) (Freedman et al. 2002). Activity and stability of the α-subunit in normoxia is regulated by oxygen-dependent hydroxylation of proline and asparagine residues by prolyl hydroxylase-2 and factor

inhibiting HIF-1 (FIH-1) (Fine and Norman 2008). Under normoxic conditions, the number of HIF-α subunits is insignificant, but in hypoxic conditions the hydroxylation is inhibited, hence the HIF-α concentrates in the cytoplasm, and is translocated to the nucleus where the process of binding with the HIF-β begins, forming a complex which activates the transcription of several genes (e.g. erythropoietin, glucose 1 transporter, angiogenic growth factors, and glycolytic enzymes) (Ribeiro et al. 2017). After exposing animal renal cells to hypoxia, it was revealed that all renal cells have the capacity to induce a transcriptional response through HIF activation. However, HIF-1α and HIF-2α are proven to be differently expressed. HIF-1α gathers in tubular epithelial cells of most nephron segments, whereas the expression of HIF-2α is located mainly in peritubular endothelial cells, fibroblasts, and glomerular cells (Eckardt et al. 2005).

HIF complex associates with HREs (hypoxia response elements) in the regulatory regions of target genes and binds the transcriptional coactivators to induce gene expression. This process is controlled by post-translational modifications, it is subjected to quick ubiquitination, proteasomal degradation, acetylation, and phosphorylation under normoxic conditions (Ke and Costa 2006). However, this process is rapidly inhibited under hypoxic conditions, resulting in an exponential increase in HIF-1α both in cultured cells and *in vivo*. The regulation of this process, at the molecular level, is the oxygen-dependent hydroxylation of proline residues Pro402 and Pro564 of N-TAD in HIF-1α by prolyl hydroxylase domain (PHD) proteins or HIF-1α prolyl hydroxylases (Figure 4) (Semenza 2002; Görlach 2009).

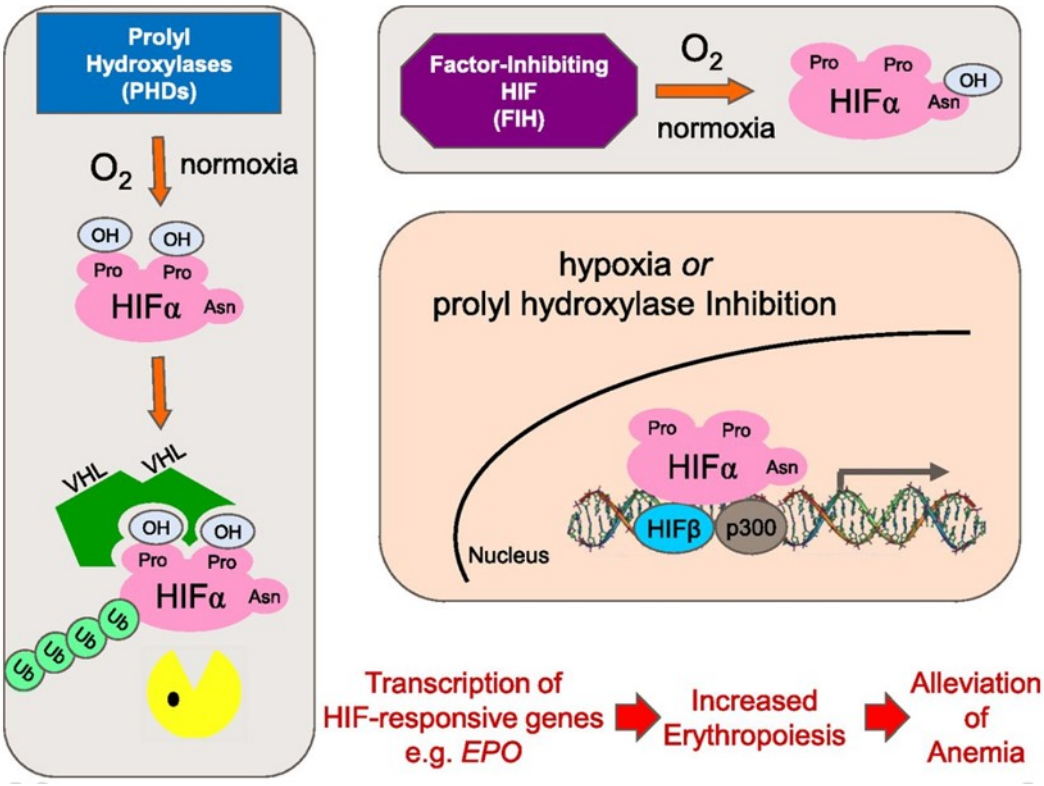

Figure 4: Schematic diagrams of the oxygen-dependent, transcriptional regulation by HIFα (Ariazi et al. 2017). VHL, von Hippel-Lindau protein

PHD proteins are a subfamily of dioxygenases, that use 2-oxoglutarate and oxygen as co-substrates, and ascorbate and iron as cofactors. In mammals, four members of this subfamily have been characterized so far: PHD1/EGLN2/HPH3, PHD2/EGLN1/HPH2, PHD3/EGLN3/HPH1, and P4HTM (Fong and Takeda 2008). PHDs consist of a conserved carboxy-terminal catalytic domain and variable amino-terminal domain. The function of the amino-terminal domain is yet to be discovered. The expression of PHDs is regulated at the transcriptional and translational levels. The first described function of the PHDs was their ability to hydroxylate human HIF-1α subunits in normoxia at two specific proline residues Pro402 and Pro564, resulting in their recognition and sequential ubiquitination by the von Hippel-Lindau protein (pVHL). This process ensures the labeling of HIF-1α for degradation by the 26S proteasome (Wong et al. 2013). After the successful hydroxylation of two proline residues of HIF-1α, pVHL captures HIF-1α in its surface pocket into which the

hydroxyproline fits perfectly; the overall binding configuration is highly specific. The pVHL associates with various proteins (e.g. elongin C, elongin B, cullin-2, ring box protein 1) to form E3 ligase complex (Hon et al. 2002). This complex is expressed in various tissues and is predominantly localized in the cytoplasm. Therefore, its transport between nucleus and cytoplasm enables HIF-1α degradation in both compartments. Binding of HIF-1α to multiprotein E3 complex causes polyubiquitination of HIF-1α leading to its degradation by the proteasome (Ke and Costa 2006).

Meanwhile, the catalytic domain of the PHDs recognizes lysine residue Lys532 located in the oxygen-dependent degradation domain of the C-TAD of HIF-1α, leading to acetylation of this lysine residue by an acetyltransferase named arrest-defective-1 (ARD1). This acetylation favors the interaction of HIF-1α with pVHL and hence destabilizes HIF-1α. Additionally, the activity of acetyltransferases is not influenced by the oxygen, meaning that ARD1 can be active and acetylate HIF-1α regardless of oxygen conditions. However, the mRNA and protein levels of ARD1 were decreased under hypoxia, causing less acetylated HIF-1α in hypoxic than that in normoxic conditions (Ke and Costa 2006). All these post-translational modifications described above regulate the stabilization of HIF-1α protein, but the stabilization alone is not sufficient for complete transcriptional activation of HIF-1. There is another mechanism controlling HIF activity through the modulation of its C-TAD. In normoxia, the asparagine residue Asn803 is hydroxylated in the C-TAD of HIF-1α by FIH-1, preventing the binding of CBP/p300, therefore reducing the activity of C-TAD, whereas, in hypoxia, the hydroxylation of Asn803 is abolished, allowing the C-TAD of HIF-1α to interact with CBP/p300 and activate the transcription of target genes (Wong et al. 2013). There are various other post-translational modifications of HIF-1α such as phosphorylation by mitogen-activated protein kinase (MAPK), as well as factors influencing HIF-1 in an oxygen-independent manner such as cytokines, growth factors or environmental stimuli, but these mechanisms are still a subject of an ongoing research (Ke and Costa 2006).

Due to the fact that various cells and organs need to adapt to the changes in oxygen supply, it is not surprising that a notable variety of the HIF-1 target genes is regulated in a tissue-specific manner. HIF-1 activates the expression of its target genes by binding to a 50-base pair HRE (hypoxia response element), which is located in the enhancer and promoter region

of the target gene, initiating varying processes (Ke and Costa 2006). HIF-1, therefore, plays an important role in erythropoiesis and iron metabolism, as well as in some aspects of cancer biology such as angiogenesis, glucose metabolism, stem cell maintenance, cell survival, proliferation, and apoptosis (Semenza 2012).

2.2.2.3. Oxidative stress

CKD-associated oxidative stress is caused by the increased reactive oxygen and nitrogen species (ROS and RNS) generation and decreased antioxidant capacity. The primary ROS produced in the human body are superoxide anion radical and hydrogen peroxide. These ROS are, in the healthy organism, well neutralized by enzymes from the superoxide dismutase family (superoxide anion radical) and catalase family (hydrogen peroxide), but they also act as signaling molecules or second messengers for numerous hormones and growth factors (Zámocký et al. 2012; Ruiz et al. 2013). However, once the ROS and RNS production exceeds the capacity of the antioxidant defense system, or this system is impaired, tissue oxidative stress, in which the ROS and RNS are converted to highly reactive and cytotoxic products (e.g.: hydroxyl radical, peroxynitrite, hypochlorous acid), which then cause tissue dysfunction and damage, develops. This process involves attacking, denaturing, and modifying structural and functional molecules, as well as activating redox-sensitive transcription factors and may result in necrosis, apoptosis, inflammation, or fibrosis. Increased production of ROS and RNS in CKD is driven by the upregulation of ROS/RNS-producing enzymes (e.g. NAD(P)H oxidase, cyclooxygenase-2, lipoxygenase, uncoupled nitric oxide synthase) or mitochondrial dysfunction. This is partly mediated by the pathological upregulation of the internal angiotensin system. In CKD, oxidative stress is often accompanied by the accumulation of inflammatory cells in the diseased kidney, in this case specifically leukocytes, which can pose as a major source of ROS. Increased ROS and RNS generation has also been proven in association with diabetes and hypertension. In fact, exposure of cultured mesangial cells to hyperglycemia showed an increased generation of ROS (Ruiz et al. 2013).

2.2.2.4. Inflammation

Inflammation is a complex defense mechanism of tissue to injurious stimuli and it is considered to be a part of the non-specific immune response. During the inflammatory response, several pro-inflammatory mediators are released into the circulating system, amongst them NO, and prostaglandin E2 (PGE_2). An integral part of this process is the enzymes, which ensure the production of NO and PGE_2, more specifically inducible form of NO synthase (iNOS) and cyclooxygenase-2 (COX-2). Several forms of NOS have been identified to this day, for instance, endothelial NOS (eNOS) and neuronal NOS (nNOS), besides iNOS. PGE_2 is produced from arachidonic acid by COXs. There are two peculiar isoforms of COX: a constitutively expressed COX-1, which provides PG in almost all tissues to maintain physiological function, and inducible COX-2, whose expression in immune cells is conditioned by the presence of infectious, injurious or differently stress-related stimuli, and produces an extensive amount of PGs that induce the inflammatory state (Zhang et al. 2009). There are two types of inflammatory processes to be distinguished – acute and chronic inflammation. The acute inflammatory process is under normal conditions self-limiting and it is typically found during an infectious challenge of the organism. In certain disorders the inflammatory process becomes continuous and chronic inflammation develops, often leading to tissue damage caused by the accumulation of pro-inflammatory mediators in the tissue (Feghali and Wright 1997), (Ferrero-Miliani et al. 2006). Typical signs of acute inflammation are the accumulation of fluid, leukocytes and cytokines (mainly interleukins (IL) 1, 6, 8 and 11, tumor necrosis factor (TNF), granulocyte-colony stimulating factor and granulocyte-macrophage colony-stimulating factor (GM-CSF), whereas the chronic inflammation is characterized by the development of specific humoral and cellular immune responses to the pathogens and/or tissue damage (Feghali and Wright 1997).

As an important contributor to the mortality and morbidity in CKD/ESRD patients, chronic inflammation is related to the cardiovascular complications, early atherosclerosis, development of malnutrition and hypoalbuminemia, as well as progression and development of anemia and mineral and bone disease (Akchurin and Kaskel 2015).

An inverse correlation between GFR and inflammation has been proven in the markers of inflammation, such as IL-1β, IL-1 receptor antagonist, IL-2, IL-6, TNF-α, C-reactive protein

(CRP) and fibrinogen (Akchurin and Kaskel 2015). Inflammation can be present in both adult and pediatric patients with CKD/ESRD. In adult CKD/ESRD patients, specific factors promoting inflammation have been found, such as advanced glycation end products (AGE), which interact with the vascular endothelial cells contributing to the development of diabetic vasculopathy, neuropathy, retinopathy, vascular inflammation and atherosclerosis. Chronic inflammation in CKD is closely related to poor cardiovascular outcomes, such as the development of CVD. The most common mechanisms linking inflammation and CVD are the attachment of macrophages to vascular endothelial cells and further endothelial dysfunction caused by inflammation-associated pro-coagulant and platelet-activating factors. Endothelial dysfunction in CKD patients is characterized by an atypical elasticity of large arteries and may be an early indicator of atherosclerosis (Silverstein 2009). Inflammation is, not only in CKD, very closely linked to oxidative stress. Due to its central role in the development and progression of CKD and related complications, the inflammatory response is an indisputable target for the development of therapeutic approaches in CKD (Akchurin and Kaskel 2015).

2.3. 3-Hydroxytyrosol

Several phytochemicals have been shown to detain anti-inflammatory activity, some of which presenting beneficial effects on renal complications (Yaribeygi et al. 2018). Importantly, the use of natural products, at safe and effective doses, may present advantages over synthetic drugs, including fewer side effects and significantly lower price, as they may be obtained from rather inexpensive and readily available matrices. An example of this type of matrices is olive oil. Olive oil is an inseparable part of the Mediterranean diet, which has many beneficial effects on human health. This diet consists of a high intake of vegetables, fruits, olive oil, and a lower intake of red meat (O´Dowd et al. 2004). Virgin olive oil, itself, is rich in phenolic compounds, e.g. 3,4-dihydroxyphenylethanol (3-hydroxytyrosol, HT), 4-hydroxyphenylethanol (tyrosol), 4-hydroxyphenylacetic acid, protocatechuic acid, caffeic acid and *p*-coumaric acid (Han et al. 2009). HT (Figure 5) is one of the key effect-carrier substances found in olives, olive leaves, and olive-derived products, such as olive oil (virgin, extra virgin). Structurally, it is a polyphenolic amphipathic compound, commonly known as

dihydroxyphenylethanol (DPE) and it is considered to be the most active olive polyphenol (O´Dowd et al. 2004). It is believed to carry powerful antioxidant, anti-inflammatory, bactericidal and bacteriostatic activity (Han et al. 2009), as well as antithrombotic activity, more specifically inhibition of low-density lipoprotein (LDL) oxidation, platelet aggregation or endothelial cells activation (O´Dowd et al. 2004), and finally anti-cancer effect on some types of cancer cells, such as colon adenocarcinoma cells (Fabiani et al. 2002) and human promyelocytic leukemia cells (Fabiani et al. 2006). Potent antimicrobial activity of this compound has been described against microorganisms, such as *Escherichia coli*, *Candida albicans*, *Clostridium perfringens*, *Streptococcus mutans, Staphylococcus aureus* or *Salmonella enterica.* The main source of HT is the hydrolysis of a polyphenolic compound oleuropein, which happens during the ripening of the olives or storage and handling of olives. The amount of HT in olive oil depends on the kind of olive tree, location of the plantation, the quality of the oil, and as importantly, on olive processing (Robles-Almazan et al. 2018).

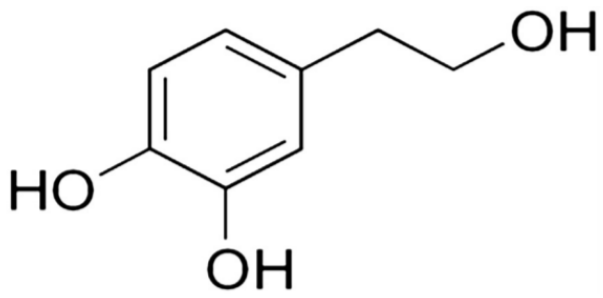

Figure 5 Structure of 3-hydroxytyrosol.

2.3.1. Metabolism of HT

HT, as a phenolic compound, is absorbed in a dose-dependent manner in the bowel and undergoes intestinal/hepatic metabolism. Its metabolites have very good distribution-abilities specifically in the muscle tissue, testis, liver, brain, and kidney. The first step of HT metabolism is oxidation and subsequent transformation into hydroxylated phenylacetic acids happening inside enterocytes, therefore gut microbiota is a notable modulator of absorption

of HT and its metabolites. The second step of HT metabolism is transformation into glucuronide, methylated, or sulphate byproducts (Figure 6). The majority of HT detected in plasma and urine is in glucuronide form, free HT can be found only at very low concentrations (Robles-Almazan et al. 2018). In rats, glucuronidation was a prevalent metabolic pathway when the dose of 1 mg/kg HT was administered, while sulfation prevailed at the dose of 100 mg/kg of HT (Rodríguez-Morató et al. 2016).

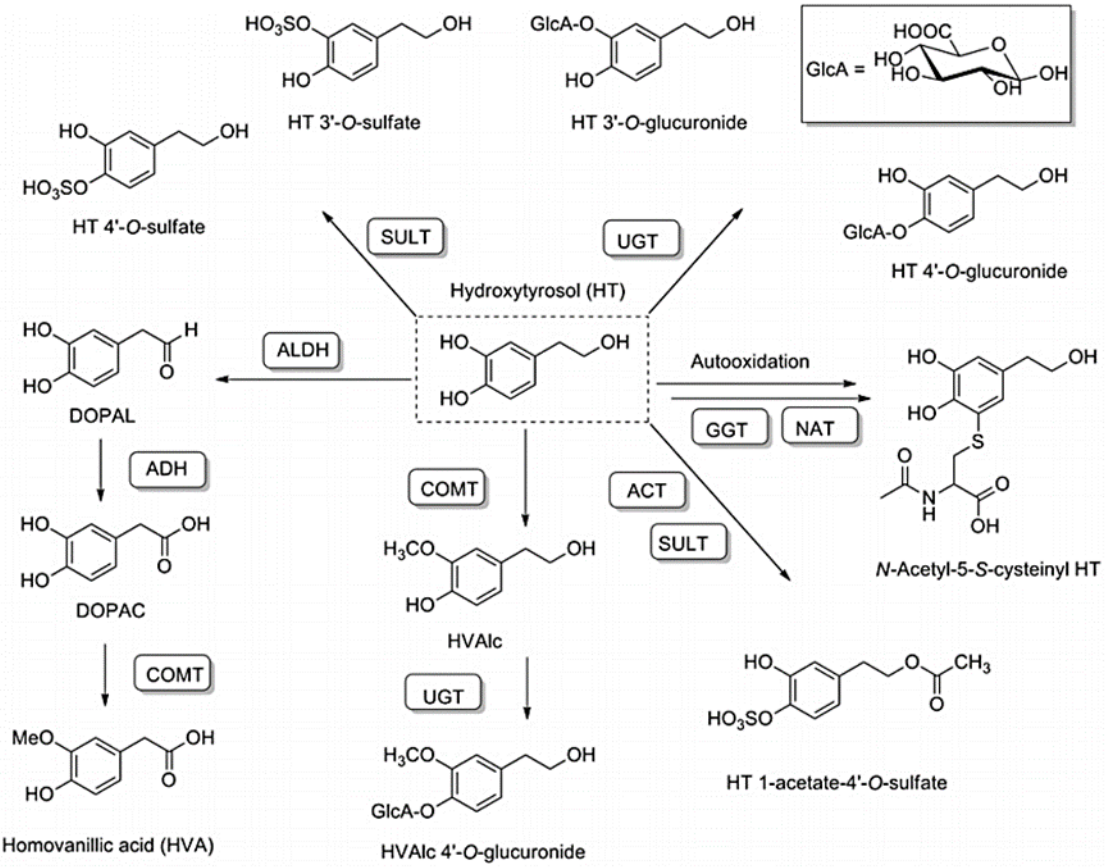

Figure 6 3-Hydroxytyrosol (HT) metabolic pathways (Rodríguez-Morató et al. 2016). ACT: O-acetyl transferase; ADH: alcohol dehydrogenase; ALDH: aldehyde dehydrogenase; COMT: catechol-O-methyl transferase; GGT: c-glutamyl transferase; GlcA: glucuronic acid; HVAlc: homovanillyl alcohol; NAT: N-acetyl transferase; UGT: UDP-glucuronosyl transferase; SULT: sulfotransferase (Rodríguez-Morató et al. 2016).

2.3.2. Anti-inflammatory and antioxidant activity of HT

As mentioned above, HT is believed to possess a relevant anti-inflammatory activity which is closely linked to its antioxidant properties. The anti-inflammatory activity of HT resides mainly in the decrease of the expression and levels of pro-inflammatory modulators (e.g. nuclear factor κB, IL-6, TNF-α) and adhesion of immune cells (e.g. monocytes and T lymphocytes) to the endothelium, preventing the endothelial dysfunction, and, in the decrease of the expression of pro-inflammatory enzymes, such as iNOS and COX-2, leading to lower circulating levels of inflammatory markers, higher expression of anti-inflammatory cytokines (e.g. IL-10) and increased activity of the antioxidant enzyme glutathione peroxidase (GPx) (Souza et al. 2017; Santangelo et al. 2018). In a study of combined consumption of white wine and virgin olive oil, the levels of inflammatory modulators (CRP and IL-6) were found significantly decreased in CKD patients when compared to baseline (Migliori et al. 2015). HT is considered to be a potent radical scavenger, thus acting as a protective factor and/or lowering the risk of oxidative stress-related conditions (Loru et al. 2009; Manna et al. 1999). HT also has the ability to inhibit free radical generation and increase plasma antioxidant activity (Bitler et al. 2005). However, the specific cellular/molecular effects, as well as the potential use of HT for the treatment of CKD and related complications is yet poorly understood and requires further consideration.

3. Aims

Renal hypoxia is a major clinical complication involved in the progression of CKD. It is therefore a potential target for the development of novel therapeutic approaches, aiming at preventing or delaying renal insufficiency.

Thus, the present work is aimed at:

- Validating a cellular model mimicking renal hypoxia using for this purpose a human cell line of renal proximal tubular cells (HK-2 cell line) exposed to cobalt chloride, an inducer of the hypoxic response.
- Evaluating the potential preventive properties of HT on the renal hypoxia, hypoxia-derived inflammation, and other related complications, such as the cell death, oxidative stress, and renal fibrosis.

4. Material and methods

4.1. Cell models

As the main organ responsible for the elimination of toxins from the organism, the kidney is a major target of uremic toxins during the progression of renal dysfunction. Furthermore, cortical renal cells, and particularly tubular proximal cells, are especially vulnerable to the hypoxic environment developed in CKD. Therefore, for the purposes of this work, a cell line of human proximal tubular cells (HK-2 cell line) and primary cultured human proximal tubular epithelial cells (HPTECs) were used. HK-2 cells retain morphological and functional characteristics of normal adult human proximal tubular epithelial cells but they are immortalized, which gives them the ability to proliferate continuously (Ryan et al. 1994). Primary cultures, on the other hand, though more representative of the *in vivo* situation, have limited proliferation capacity and are harder to obtain. Therefore, a preliminary study was performed to compare the two cell models in terms of the basic response (cell death) to the induction of hypoxia.

The optimal method for inducing hypoxia is through a low-oxygen environment. However, a hypoxic chamber, or at least a CO_2 incubator with a regulated level of oxygen are needed. The CO_2 incubator method is however not the best for many types of experiments, because oxygen re-enters the chamber at each opening, and even though, the hypoxia incubator enables changing of the medium and other manipulation with cells in a continuous hypoxic environment, it is very expensive and therefore not affordable in many laboratories. For these reasons, we opted for chemically induced hypoxia, with exposure of cells to cobalt chloride ($CoCl_2$), which allows a strong and sustained stabilization of HIF-1α and HIF-2α when cells are exposed under normal oxygen levels, comparable to alternative hypoxia mimics. Generally accepted knowledge about $CoCl_2$ induced hypoxia is that Co^{2+} substitutes Fe^{2+} (an important cofactor of the activation of PHDs) in PHDs. This leads to blocking of the PHDs activity, disturbing the hydroxylation of HIF-1α and subsequently inhibiting the ubiquitin-dependent 26S proteasomal degradation pathway. $CoCl_2$ also shows inhibitory effect on FIH-1, thus increasing the transcriptional activity of HIF-1 factors (Muñoz-Sánchez and Chánez-Cárdenas 2018).

4.1.1. Isolation and primary culture of human proximal tubular epithelial cells

The normal/functional cortical tissue used for the isolation of HPTECs was obtained from consenting patients with renal carcinoma undergoing radical nephrectomy. The tissue was taken from the pole distant to the tumorous tissue and was placed into a sterile test tube with ice-cold serum-free medium and processed promptly, as thoroughly described below, following the protocol of Valente et al. 2011. All procedures were carried out using aseptic technique inside a laminar flow chamber. The sample was cut in pieces, placed in a tube and washed 3 times with phosphate-buffered saline (PBS) to remove as much blood as possible. Remains of fat and capsule were removed, using a surgical scalpel, and discarded. The rest of the sample was carefully minced using a surgical scalpel, and transferred into a glass-jacketed flask, maintained at 37°C with warmed water circulating through the flask's jacket. A collagenase solution (1mg/mL) prepared in a pre-warmed serum-free medium was added to the flask and the process of digestion was initiated under magnetic agitation for 20 minutes at 37°C. The suspension was sequentially passed through sterile 100, 70, and 40 μm sieve, allowing the elimination of undigested tissue, tubular fragments and glomeruli, respectively. The final filtrate was collected into a sterile test-tube and centrifuged at 400×g for 5 minutes at 4°C in a refrigerated centrifuge. The supernatant was discarded, and the cell pellet was resuspended in PBS, continuing the washing process 2 more times following the same conditions. The supernatant was then discarded, and cells were resuspended in the complete growth medium, prepared as follows:

- 1 L of Dulbecco′s Modified Eagle′s Medium: Nutrient Mixture 12 (DMEM/F12)
- 10% fetal bovine serum (FBS)
- 1% penicillin/streptomycin (final concentration: 50 U/mL/50 mg/mL)
- 1% amphotericin B (final concentration: 2.5 μg/mL)
- 0.1% human transferrin (final concentration: 5 μg/mL)

The proximal tubular cells obtained with this procedure were counted using the trypan blue counting protocol and subsequently cultured in collagen-coated 75 cm^3 flasks at 50 000 cells/cm^2 density.

HPTECs can be subcultured for a maximum of 4 passages (Figure 7) in order to guarantee the preservation of the morphological/functional features of the isolated cells.

4.1.2. The routine protocol for culture of HK-2 cells

For experimental purposes, frozen HK-2 cells, stored at -80°C in freezing medium (culture medium with 20% FBS and 10% dimethylsulfoxide, DMSO), were thawed and grown in 75 cm^3 cell-culture flasks in growth medium, prepared as follows:

- 1 L of DMEM/F12 medium
- 10% FBS
- 1% penicillin/streptomycin (final concentration: 50 U/mL/50 mg/mL)

The frequency of medium changing was based on the overall state of the cells checked under an inverted microscope, though never exceeding 48 hours (Figure 8). The cells in culture flasks were stored in a thermoregulated cell culture incubation chamber at 37°C, and a 5% CO_2 atmosphere. The processes of changing the medium, passing the cells, or plating the cells were all handled in a laminar flow cabinet, which was, along with the used material, sterilized with a UV-C germicidal lamp beforehand for 20-30 minutes.

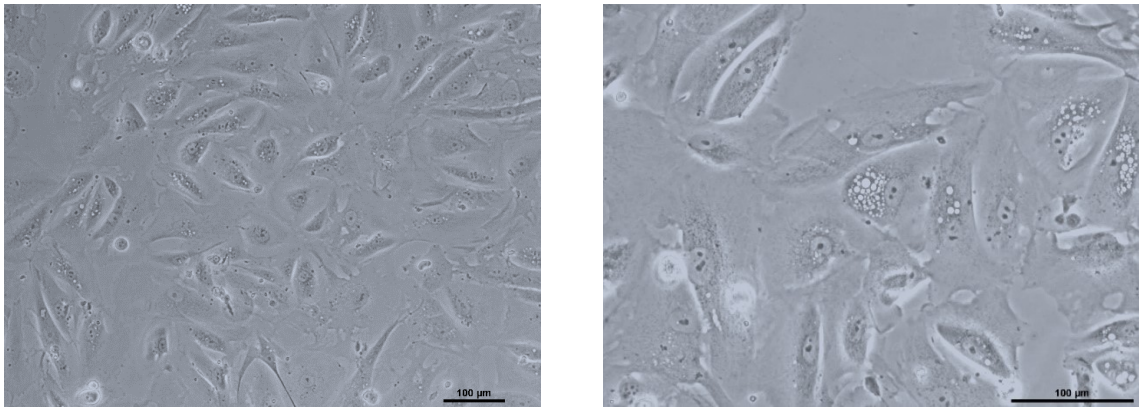

Figure 7 HPTECs in culture medium under microscope, 100x (left) and 200x (right) magnification.

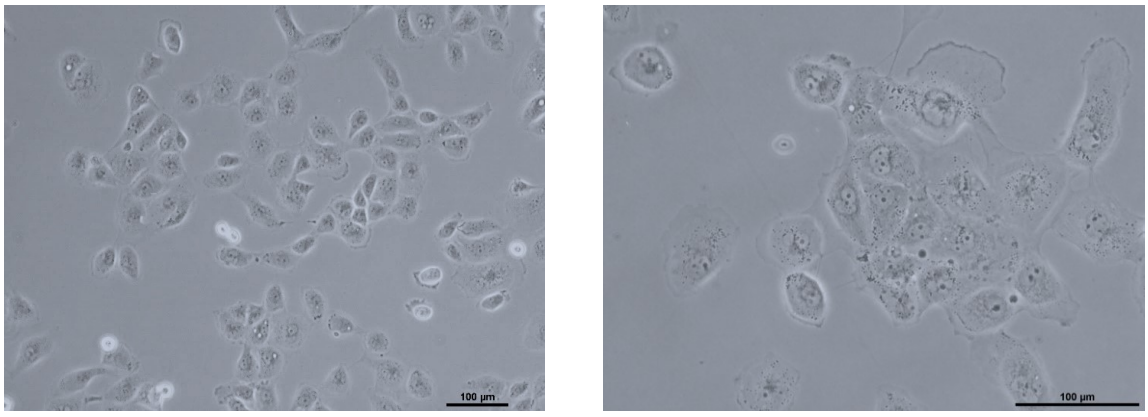

Figure 8 HK-2 cells in culture medium under microscope, 100x (left) and 200x (right) magnification.

4.1.3. Cell counting

For counting the cells, the method of trypan blue exclusion using a Neubauer hemocytometer chamber was used. The Neubauer hemocytometer is divided into 9 squares (1 mm^2 each), each of those squares is subdivided into 16 smaller squares (0.4 mm^2 each). For very simple quantitation of cell viability, the trypan blue exclusion test was used. The principle of this method is the ability of healthy, viable cells with intact cell membrane to exclude certain dyes, such as trypan blue, meaning that these cells will appear clear under the microscope, whereas dead (nonviable) cells tend to take up the dye into the cytoplasm, therefore appearing dark blue (Strober 2015).

Before each use, the Neubauer chamber was cleaned with distilled water and patted dry with a paper cloth. The 500 µL of cell suspension and 50 µL of trypan blue solution were mixed and the homogenized cell suspension with trypan blue solution was carefully added under the thin-glass coverslip until evenly distributed, without overflowing the chamber. The chamber with the sample was placed in an inverted microscope and counted. The cells were counted in a snake-like pattern, only counting the cells located in the larger corner squares, and the cells touching two selected sides of the squares (e.g. right and bottom) and calculated. For calculating the number of cells per 1 milliliter, the following formula was used:

$$c = \frac{x}{a} \times DF \times 10^4$$

c – number of cells per 1 mL

x – cell number counted from the Neubauer hemocytometer chamber

a – number of squares counted (2 chambers X 4 squares)

DF – dilution factor (1.1)

10^4 – recalculation of the number of cells to 1 mL (1 000 mm^3), considering the volume of each square of the chamber (0.1 mm^3)

4.1.4. Cell subculture

HK-2 cells are adherent cells that grow in a monolayer. Therefore, after reaching a certain level of confluency (80%) in the culture flask, cells need to be subcultured. This process is often referred to as passaging cells, and it enables keeping the cells growing in cultured conditions for extended periods of time. All the reagents used for passaging the cells were pre-heated to 37°C before use. Firstly, the used medium was discarded from the culture flask and cells were washed two times with PBS, then 3 mL of 0.25% trypsin-EDTA was added to detach the cells from the surface of the flask and left on the cells for approximately 3 minutes. After this time cells must be checked under the microscope to see the level of detachment. Once the cells were floating and created a cell suspension, the enzyme was inactivated by adding 12 mL of the growth medium and cells were counted using the method in the Neubauer hemocytometer chamber described above. The rest of the suspension was divided using 1:3 or 1:4 ratio (depending on the number of cells counted) to reach the desired density, to a new 75 cm^3 culture flasks with fresh growth medium.

4.1.5. Cell plating

Once the cells reached an adequate passage required for the experiment, they were plated at a density of 50 000 cells/cm^2, into 96-well plates (16 000 cells/well/100 µL), 24-well plates (95 000 cells/well/250 µL), or 6-well plates (480 000 cells/well/1 mL), depending on the number of cells required for each assay.

4.2. Viability assessment through the MTT reduction assay

HK-2 cells were plated in 96-well plates, and after attaching overnight, the growth medium was aspirated and $CoCl_2$ solution was added in triplicates. The concentrations of $CoCl_2$ solution used in this experiment were 0.002, 0.005, 0.02, 0.05, 0.1, 0.2, 0.4, 0.5, 0.6, 0.8, 1.0, 1.2, 1.5, 2, 5, 10 mM in serum-free medium (to avoid eventual formation of adducts with FBS proteins), prepared fresh before use. The 100 µL of this solution was added to each well, carried out in triplicates as shown in Figure 9. The plates were then incubated for 24

hours at 37°C and 5% CO_2 atmosphere. After 24 hours, the $CoCl_2$ solution was aspirated and the MTT reduction assay was performed, by incubating cells with 100 µL per well of 0.5 mg/mL MTT for 1 hour at 37°C and 5% CO_2 atmosphere. The MTT reduction assay is a widely used colorimetric method for an indirect evaluation of the viability of cells based on their mitochondrial activity, by the ability of viable cells to reduce the yellow MTT ([3-(4,5-dimethylthiazol-2-yl)-2,5-diphenyl tetrazolium] bromide) to purple formazan crystals, which are, for better evaluation, then dissolved using DMSO solution and absorbance is measured at 540 – 720 nm (Van Meerloo et al. 2011). After 1-hour incubation, the now reduced MTT solution was removed and 100 µL of DMSO was added to the wells and left on the shaker for 15 minutes, to dissolve the purple formazan crystals. Any bubbles created during the process of shaking were punctured with a sterile needle, to ensure no interference in absorbance values. Absorbance was then monitored at 550 nm directly in the plate using a multi-plate reader and the results were exported to a Microsoft Excel file and further evaluated. Data were normalized to negative (no $CoCl_2$, serum-free medium only, therefore 0% cell death) and positive (1% Triton X-100 solution, inducing 100% cell death) control.

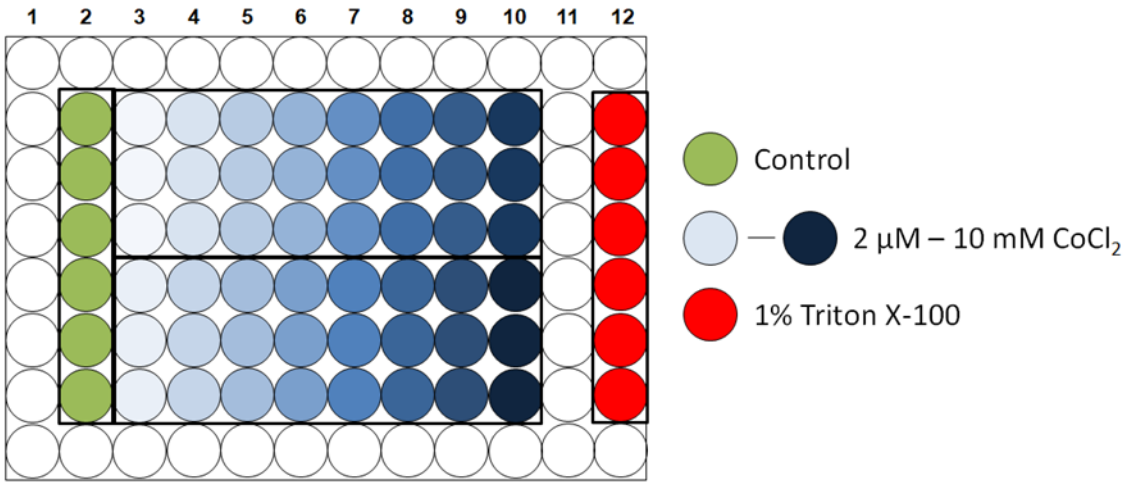

Figure 9 The template of exposure to various concentrations of $CoCl_2$ used for the MTT assay.

From the concentration-response curves obtained from the previous assay, the concentrations inducing specific inhibitory effects of cell viability (Inhibitory Concentrations, ICs) were interpolated, namely the concentrations inducing 1, 5, 10, 20, 25, and 50% of cell death (IC_{01}, IC_{05}, IC_{10}, IC_{20}, IC_{25}, and IC_{50}).

Once an adequate IC of $CoCl_2$ for the induction of hypoxia was determined, the MTT assay was also performed to evaluate the potential preventive effects of HT on the decrease in viability induced by $CoCl_2$. For this purpose, after attaching overnight, cells were exposed to a safe and physiologically relevant concentration of HT, i.e. 5 µM, for 1 hour at 37°C, followed by a 24-hour exposure period with IC_{25} $CoCl_2$/5 µM HT, as depicted in the template pictured in Figure 10.

Data were again normalized to negative (serum-free medium only) and positive (1% Triton X-100) control of cell death.

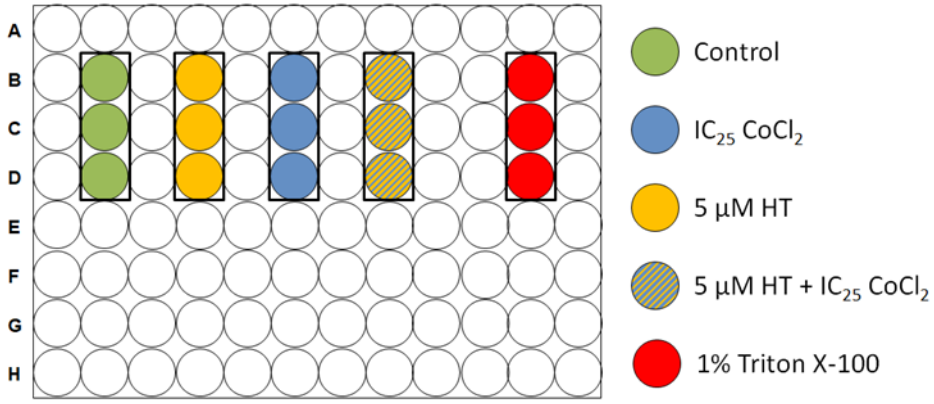

Figure 10 The template used for exposure to the chosen IC_{25} $CoCl_2$ and/or HT.

4.3. Evaluation of oxidative stress status

4.3.1. Measurement of ROS and RNS production

ROS and RNS includes a number of molecules (e.g. hydrogen peroxide, oxide anion, nitric oxide, hydroxyl radical, etc.) with physiological functions. However, when produced at high amounts, they can be very damaging as they are considered to be very unstable and highly reactive molecules. This peculiarity is also used for the detection of ROS and RNS, which

relies on measuring the end products of their reactions with particular substances. These end-products can be measured by changes in their properties such as fluorescence, luminescence, or color (Jambunathan 2010). For the purposes of our experiment, 2′,7′-dichlorodihydrofluorescein diacetate (DCFH-DA) was used to probe samples for 1 hour, prior to the incubation with the test compounds. DCFH-DA is a nonfluorescent compound, which can pass through cell membranes. Once it reaches the cytoplasm, cell esterases remove the acetates and produce 2′,7′-dichlorodihydrofluorescein (DCFH), which is not permeable due to its polarity. DCFH is easily oxidized by ROS and RNS to 2′,7′-dichlorofluorescein (DCF), a highly fluorescent compound (excitation 485 nm, emission 530 nm).

The HK-2 cells were plated in 96-well plate, using 100 µL of complete medium, and left attaching at 37°C overnight. The complete medium was then aspirated and 100 µL of 50 µM DCFH-DA solution in serum-free medium was added to each well and left incubating for 1 hour at 37°C. At the end of the incubation period, the supernatant was discarded, and cells were incubated with 100 µL per well of the test compounds, carried out in triplicates. For testing the effects of HT on the hypoxia-elicited oxidative stress, cells were co-exposed with 5 µM HT and 50 µM DCFH-DA for 1 hour. The template for this experiment was the same as pictured in Figure 10. After 24 hours of exposure, the fluorescence was monitored using a fluorescence plate reader (baseline 485 nm excitation, 530 nm emission). The results were exported to a Microsoft Excel file and further analyzed, normalized to controls (serum-free medium only), and presented as fold-increase over control.

4.3.2. Measurement of GSH/GSSG levels

Glutathione (GSH), as a ROS scavenger, belongs to the primary antioxidant defense of the organism. GSH takes part in both enzymatic and nonenzymatic reactions. In these reactions, GSH is converted to glutathione disulfide (GSSG), its oxidized form. High levels of GSSG in the organism stimulate the activity of glutathione reductase (GR), which transforms GSSG back to GSH, and helps to preserve a steady balance of GSH and GSSG. The GSH/GSSG ratio is a satisfactory oxidative stress indicator. This assay is based on the reaction of GSH

with Ellman´s reagent (5,5'-dithiobis-(2-nitrobenzoic acid), DTNB), which produces TNB chromophore (with maximal absorbance at 412 nm), and an oxidized glutathione-TNB complex (GS-TNB). The rate in which GS-TNB is formed is proportional to the concentration of GSH in the sample. The GS-TNB complex is then reduced by GR in the presence of NADPH, which results in the recycling of GSH back into the reaction. The amount of GSH acquired with this reaction represents the sum of reduced and oxidized GSH in the sample. Estimating the amount of GSSG is difficult as GSH is rapidly oxidized into GSSG, causing alteration of the GSH/GSSG ratio in the sample. Therefore, it is important to measure the GSSG immediately to avoid rapid GSH oxidation. The cells are treated with 2-vinylpyridine, which covalently binds to the GSH, but not to the GSSG. The excess of the 2-vinylpyridine is neutralized with triethanolamine. The GSSG is then determined by monitoring the kinetics of conversion of NADPH spectrophotometrically (Rahman et al. 2007).

HK-2 cells were plated in a 6-well plate, using 1 mL of complete medium per well with the desired density (480 000 cells/well). After attaching overnight, cells were exposed to the test compounds, as depicted in Figure 11. Afterward, the supernatant was discarded and 250 µL of 5% $HClO_4$ was added to each well and incubated on ice for 20 minutes. Cells were then scraped off with a cell scraper, collected into the test tubes, and centrifuged at 13 000×g for 5 minutes at 4°C. The supernatant was transferred into new test tubes and used for further GSH/GSSG evaluation. This process allowed us to obtain samples without protein prior to the quantification of GSH/GSSG. The precipitated protein was then resuspended in 250 µL of 1 M NaOH and stored at -20°C until further use.

For the purposes of the determining total GSH, 100 µL of standard/sample with 100 µL of 0.76 M $KHCO_3$ were placed in a test tube, vortexed several times with opening and closing of the lid, and centrifuged at 11 000×g, for 5 minutes at room temperature. In 96 well plates, 100 µL of standard/sample with 65 µL of reagent solution in phosphate buffer (0.1 M, pH 7.4) were first incubated for 15 minutes at 30°C. After the incubation period, 40 µL of GR was added quickly to each well, and the absorbance was monitored at 415 nm for 3 minutes. The standard concentration range of GSH used was 0.78 – 50 µM. All reagents were covered in aluminum foil to eliminate light exposure and subsequent oxidation.

To determine the amount of GSSG, 100 µL of standard/sample with 5 µL of 97% 2-vinylpyridine was agitated for 1 hour at room temperature inside a flow hood. The 100 µL of standard/sample with 100 µL of 0.76 M $KHCO_3$ were vortexed and then centrifuged at 11 000×g for 5 minutes at room temperature. In 96 well plate, 100 µL of standard/sample and 65 µL of reagent solution in GSH/GSSG buffer were incubated for 15 minutes at 30°C. GR was added quickly and absorbance was monitored at 415 nm for 3 minutes. Standard of GSSG was used in the following range of concentrations: 0.19 - 12 µM. All reagents were covered in aluminum foil to eliminate light exposure and subsequent oxidation.

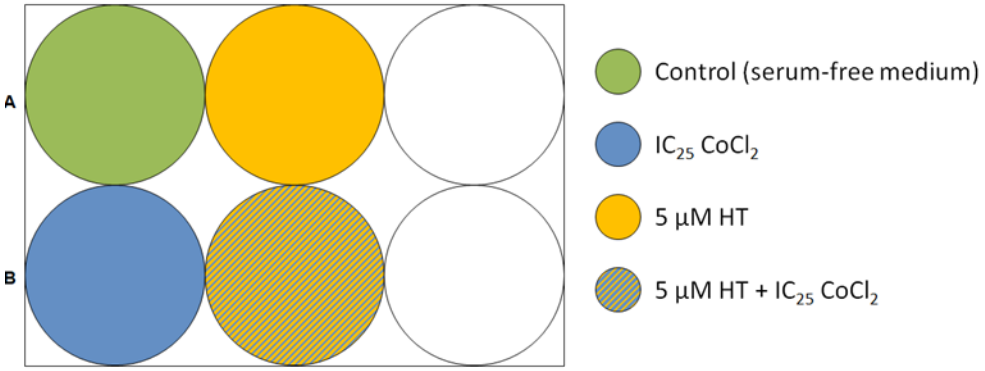

Figure 11 Template for exposure to IC_{25} $CoCl_2$ and/or HT used in GSH/GSSG assay and Bradford protein quantification method.

4.4. Protein quantification using the Bradford assay

This assay is a very quick and accurate method for quantification of protein in various samples. It is based on the binding of Coomassie Blue G250 dye to protein, most strongly to amino acids, such as arginine and lysine, to lesser extent histidine, tryptophan, and phenylalanine (Kruger 2002). Bradford reagent was prepared by dissolving Coomassie Brilliant Blue G250 in 95% ethanol, 85% phosphoric acid, and distilled water. The solution was left to rest overnight, filtered in a dark flask the next day, and stored safe from light. Before every use, it was filtered through filter paper again. The protein standard range used in this assay was 5 – 50 µg/mL bovine serum albumin (BSA) prepared in distilled water.

Samples of HK-2 cells were acquired from the process of deproteinization of the samples used in the GSH/GSSG assay mentioned above, which were dissolved in 1 M NaOH, and diluted in water for the purpose of this assay. The Bradford Reagent was filtered through filter paper and 200 µL were added in each well. The plate was agitated for 10 seconds to assure homogenization and absorbance was monitored by a plate reader at 595 nm (reference reading at 690 nm). The calibration curve was traced from standards, and the concentration of the sample was interpolated from the curve.

4.5. Flow cytometric analysis of cellular hypoxia

Flow cytometry is a highly sophisticated instrumental method which allows measuring of multiple characteristics of cells or other particles. A sample of cells/particles is suspended in a fluid and injected into the flow cytometer. The sample flows uniformly through a laser beam, where the light scattered is characteristic for the cells/particles and their components. Cell-labeling is often performed before analysis, either with fluorescent dyes or antibodies. This labeling can be targeted to extracellular molecules located on the surface of the cells or intracellular molecules located inside the cells. Flow cytometry allows us to analyze thousands of particles per second in real-time. It is, therefore, considered a quick and highly effective instrumental method of analysis of cell-characteristic (Adan et al. 2017). To select the best IC of $CoCl_2$ to induce the renal hypoxia cell model, the Hypoxia Green (HG) reagent (Thermo Fisher Scientific, Massachusetts, USA) was used to label HK-2 cells, which have previously been exposed to various ICs of $CoCl_2$, allowing the determination of the level of hypoxia induced by this compound at each IC. The HG reagent is an antibody independent reagent, used for detecting low oxygen levels in live cells. After penetrating the membrane of cells, this probe releases rhodamine as oxygen levels decrease, resulting in a fluorogenic response. This fluorogenic response is then monitored in a flow cytometer using a 530/30 nm emission filter. After incubation of HK-2 cells cultured in 24-well plates with $CoCl_2$, the supernatant was discarded and cells were trypsinized and collected in the complete medium into the test tubes. Cells were then centrifuged at 400×g for 3 min at room temperature, and after discarding the medium, a solution of HG reagent prepared in serum-free medium was added to each tube, and samples were incubated for 2.5 hours at 37ºC. After this period of

incubation, 20 000 events from each sample were analyzed in a BD Accuri C6 flow cytometer (BD Biosciences, California, USA), using the FL-1 filter (530 nm). Data was presented as % of FL-1 fluorescence over control (cells exposed just to serum-free medium).

4.6. Analysis of the formation of acidic vesicular organelles through fluorescence microscopy and flow cytometry

Autophagy is characterized by increased formation of acidic vesicular organelles (AVOs), may they be lysosomes or autophagolysosomes. These AVOs can be labeled using acridine orange (AO), a weak base that accumulates in acidic spaces where it emits yellow-to-red fluorescence; when intercalated with the DNA, AO emits green fluorescence. The fluorescence of this dye may be observed under a fluorescence microscope or quantified through flow cytometry. For observation purposes, cells exposed to medium, HT, $CoCl_2$, or the combination of HT and $CoCl_2$ were exposed to a solution of 0.5 µg/mL AO for 15 min at 37ºC, rinsed twice with PBS, and observed under an inverted fluorescence microscope. For quantification of AVOs, after exposure, cells were trypsinized and collected into tubes, and incubated with 0.5 µg/mL AO, rinsed twice by centrifugation at 400×g for 3 min and analyzed in a BD Accuri C6 flow cytometer (BD Biosciences, California, USA), using the FL-3 filter (670 nm). Data was presented as % of AO^+ events over control (cells exposed just to serum-free medium).

4.7. Gene expression analysis by quantitative polymerase chain reaction (qPCR)

A qPCR is a very potent tool for quantitative nucleic acid analysis. It allows amplifying small amounts of DNA or mRNA for various experiments. The amount of product formed in qPCR is monitored during the ongoing reaction by measuring the fluorescence of probes and dyes added to the samples. The fluorescence of these probes is proportional to the amount of product formed. To obtain a particular amount of DNA molecules, the number of amplification cycles required is being registered. Today, a qPCR is considered to be a quick, relatively cheap, and foremost efficient method for pathogen detection, gene expression

analysis, single nucleotide polymorphism analysis and protein detection by real-time immune-PCR (Kubista et al. 2006).

First, to evaluate the effect of $CoCl_2$ as an inducer of hypoxia in human proximal tubular cells, HK-2 cells were exposed to various ICs of $CoCl_2$, as previously determined by the MTT assay. These ICs were used for the analysis of gene expression of different hypoxia-related mediators by qPCR. For this assay, cells were plated in 24-well plates and exposed with 300 µL of $CoCl_2$ solutions in duplicates (Figure 12). After the selection of the most adequate IC of $CoCl_2$ (the highest expression of hypoxia markers) for the evaluation of the preventive effect of HT on the induced renal hypoxia, HK-2 cells were pre-exposed to 5 µM HT for 1 hour prior to the 24 hours co-incubation period of the selected IC of $CoCl_2$ and 5 µM HT (Figure 13). Besides hypoxia markers, in order to further unveil the mechanisms of action of HT on renal hypoxia, samples obtained from this assay were also analyzed for the expression of genes related to the inflammatory response, fibrosis, and cell death.

For this purpose, exposed cells were collected and lysed with TriPure Isolation Reagent, an RNA isolation solution. RNA was extracted from the samples by liquid extraction with chloroform, followed by precipitation with isopropanol, and washing of the RNA pellet with 75% ethanol. The RNA was then dried, resuspended in RNase-free water and quantified using a Nanodrop spectrophotometer (Thermo Fisher Scientific Nanodrop 1000, Massachusetts, USA) at 260 nm. The conversion of RNA into complementary DNA (cDNA) was performed using the Xpert cDNA Synthesis Kit (GRiSP, Porto, Portugal), according to the manufacturer's instructions. This kit contains reverse transcriptase that mediates the conversion, RNase inhibitor for protection of template from degradation, reaction buffer, a mix of deoxynucleotide triphosphates (dNTPs = dATP + dCTP + dGTP + dTTP), and oligo$(dT)_{20}$ primer, from which the cDNA synthesis is initiated. RNA conversion was performed at 50°C, using a thermocycler (Thermal Cycler T100, Bio-Rad Laboratories, California, USA).

The synthesized cDNA was then used as a template for gene analysis by qPCR (StepOnePlus™ Real-Time PCR System, Thermo Fisher Scientific, Massachusetts, USA), using the Xpert Fast SYBR 2× Mastermix (GRiSP, Porto, Portugal), which is a buffer containing polymerase and dNTP mix. The conditions of analysis were as follows: after an

initiating 3-min cycle at 95°C, extension and annealing of the template was achieved over 40 cycles of 5 sec at 95°C and 30 sec at the optimal annealing temperature (determined *a priori* for each pair of primers), finalizing with dissociation at 95°C for 15 sec, and a melting analysis of the amplified product.

The expression of the following genes was assessed, with the sequences of their primers, shown in Table 2:

- Hypoxia-related genes - *HIF1A* (coding for HIF-1α), *ARNT* (coding for HIF-1β), *SPP1* (coding for osteopontin, OPN) and *GAPDH* (coding for glyceraldehyde-3-phosphate dehydrogenase, GAPDH)
- Inflammation-related genes – *IL6* (coding for IL-6), *TNF* (coding for TNF-α), *NFKB1* (coding for NF-κB), *PTGS2* (coding for COX-2) and *CCL2* (coding for monocyte chemoattractant protein 1, MCP-1)
- Fibrosis-related genes – *TGFB1* (coding for transforming growth factor β, TGF-β) and *IL1B* (coding for IL-1β)
- Cell-death related genes – *CASP3* (coding for caspase 3) and *SQSTM1* (coding for p62)

Gene expression of *TUBA1* (coding for α-tubulin) was also measured as a housekeeping gene, and all data were normalized for its expression.

Table 2 The sequences of the used primers.

Gene	Forward primer (**5'->3'**)	Reverse primer (**5'->3'**)
HIF1A	CCCTAACTAGCCGAGGAAGA	CACAAATCAGCACCAAGCAG
ARNT	CTTCTTGGATTAGCCGTCCC	TCTCAAGATTGGAGGGAGCA
SPP1	GCCACAAGCAGTCCAGATTA	TTTTGGGGTCTACAACCAGC
GAPDH	TATGACAACAGCCTCAAGAT	GAGTCCTTCCACGATACC
IL6	GGAGACTTGCCTGGTGAAAA	GTCAGGGGTGGTTATTGCAT
TNF	CTCAGCCTCTTCTCCTTCCT	AGGGTTTGCTACAACATGGG
NFKB1	TGGTGGGAAAACACTGTGAG	ATAGCCCCTTATACACGCCT
PTGS2	CCCTTGGGTGTCAAAGGTAAAA	AACTGATGCGTGAAGTGCTG
CCL2	GAGAGGCTGAGACTAACCCA	GGCATTGATTGCATCTGGCT
IL1B	CATTGCTCAAGTGTCTGAAGC	CGGAGATTCGTAGCTGGATG
TGFB1	CTCGCCAGAGTGGTTATCTT	GGTAGTGAACCCGTTGATGTC
CASP3	TAGATGGTTTGAGCCTGAGC	GCTTCACTTTCTTACTTGGCG
P62	GGAGTCGGATAACTGTTC	GATTCTGGCATCTGTAGG
TUBA1	CTGGAGCACTCTGATTGT	ATAAGGCGGTTAAGGTTAGT

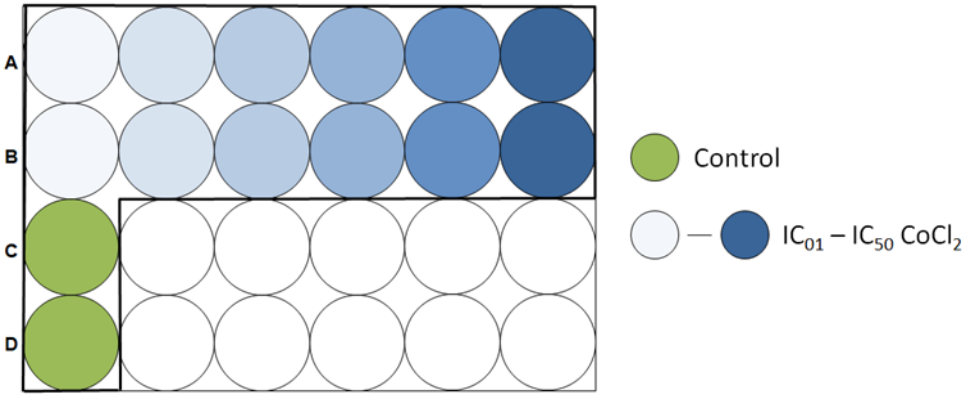

Figure 12 Template for exposure of HK-2 cells to various ICs of $CoCl_2$, used for quantification of gene expression of hypoxia-related markers.

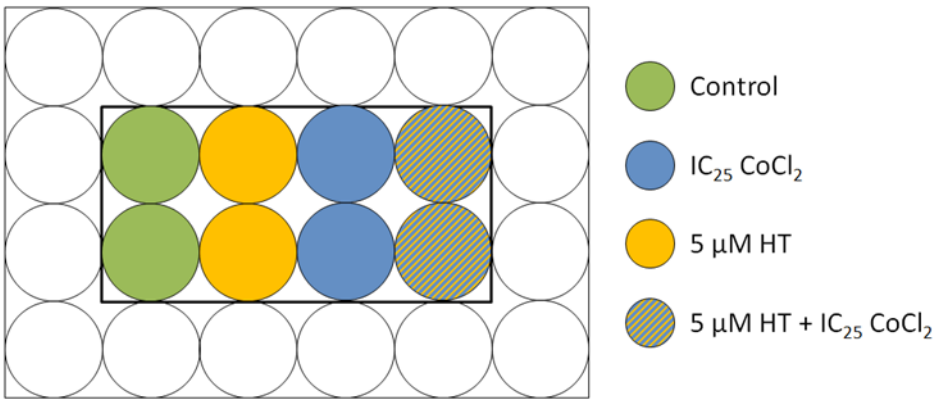

Figure 13 Template for exposure of HK-2 cells to IC_{25} of $CoCl_2$ and/or 5 µM HT, used for quantification of gene expression of hypoxia-, inflammation-, fibrosis- and cell death-related markers.

4.8. Statistical Analysis

All statistical analysis was performed using GraphPad Prism 7 software. The logistic function was employed for the nonlinear fit curves of normalized MTT reduction data; data are presented as mean ± 95 % confidence interval. The IC_x values for each cell line were interpolated from the traced fits, and a global fit analysis was performed to compare cell models. For the other quantitative assays, results are presented as mean ± standard error of the mean. The normality of data distribution was assessed through the Shapiro-Wilk normality test. Multiple comparisons between conditions were performed by one-way ANOVA analysis followed by the Fisher's LSD post-hoc test for normally distributed data, or by the Kruskal-Wallis test followed by the Uncorrected Dunn's test otherwise. For qPCR gene analysis data, multiple comparisons between test conditions were evaluated by two-way ANOVA analysis followed by the Fisher's LSD post-hoc test. Results are from 2 to 7 independent experiments, depending on the assay, and, therefore, several assays require the conduction of more independent experiments for confirmatory purposes. *P* values lower than 0.05 were considered statistically significant.

5. Results

5.1. Effect of $CoCl_2$ on cell viability of HK-2 cells and HPTECs

As depicted in Figure 14, a wide range of concentrations of $CoCl_2$ (from 2 µM to 10 mM) was tested in order to define the effect of exposure to $CoCl_2$ on the viability of both HK-2 cells and HPTECs.

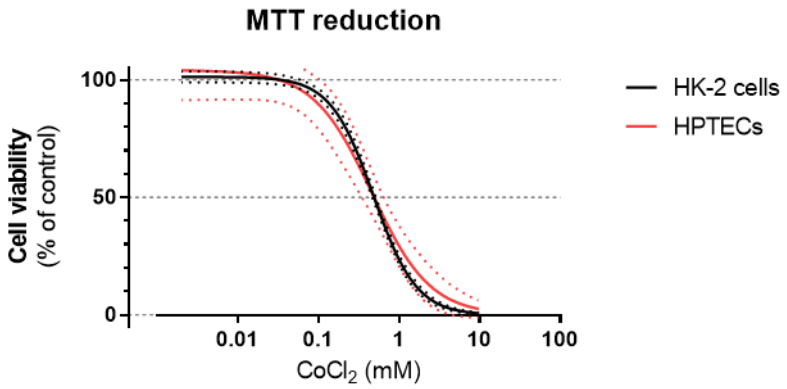

Figure 14 Concentration-response curve on cell viability of cells using the MTT assay ($CoCl_2$ in HK-2 cells, HPTECs)

The purpose of this experiment was to determine which concentrations of $CoCl_2$ are considered safe and which hazardous. The highest concentration, 10 mM $CoCl_2$, induced approximately 100 % death in both cell models. By conducting this assay on both HK-2 cells and HPTECs, we managed to show that there is no significant difference between the nonlinear fits of two cell models ($p = 0.1618$ for the global fit of HK-2 cells *versus* HPTECs), and interpolate the concentrations of $CoCl_2$ that induce a specific inhibitory effect on the cell viability, used in further experiments in HK-2 cells (Table 3).

Table 3 The comparison of ICs of $CoCl_2$ in HK-2 cells and HPTECs.

	[$CoCl_2$] (mM)						**Overall fit**
	IC_{01}	**IC_{05}**	**IC_{10}**	**IC_{20}**	**IC_{25}**	**IC_{50}**	***p* value**
HK-2 cells	0.048	0.092	0.136	0.215	0.254	0.491	0.1618
HPTECs	0.039	0.065	0.098	0.169	0.209	0.492	

5.2. Effect of $CoCl_2$ as a hypoxia inducer in HK-2 cells

In order to determine the most adequate $CoCl_2$ concentration to induce renal hypoxia, the intracellular oxygen levels of HK-2 cells exposed to different ICs (indicated in Table 3) were evaluated through flow cytometry using the HG reagent. The results are presented in Figure 15.

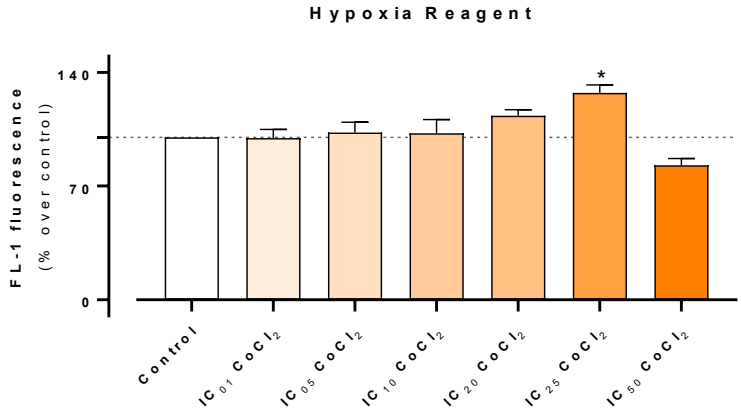

Figure 15 Flow cytometry of HG reagent-labeled HK-2 cells exposed to various ICs of $CoCl_2$. * $p < 0.05$ *versus* control.

When compared to control, only IC_{25} $CoCl_2$ was able to induce a significant increase in green fluorescence, i.e. a significant decrease in oxygen levels (127.4 ± 4.7 % of fluorescence over control). The fluorescence decreased in IC_{50}, probably due to the notable effect on cell viability, that this concentration already possesses.

In this experiment, we continued to determine the best IC of $CoCl_2$ to use as an inducer of hypoxia for further experiments. In order to do this, we chose 4 hypoxia-related genes: *HIF1A*, *ARNT*, *GAPDH*, and *SPP1* compared to the control sample with complete medium only. As shown in Figure 16, we observed an increase in the expression of *HIF1A*, *GAPDH*, and *SPP1* up to IC_{20}/IC_{25}, though not significantly for *HIF1A*. For *GAPDH*, this increase was significant for all tested ICs ($p < 0.01$), while for *SPP1* only in IC_{20} and IC_{25} we observed an increase with statistical significance ($p < 0.05$).

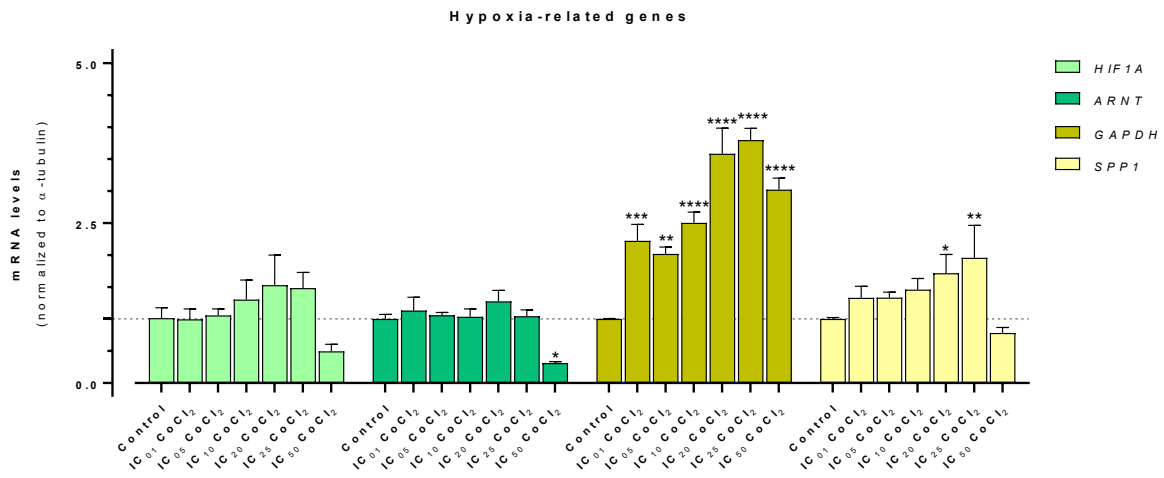

Figure 16 Study of gene expression of hypoxia-related markers on HK-2 cells, exposed to various ICs of $CoCl_2$. Data was normalized for the expression of *TUBA1*. * $p < 0.05$, ** $p < 0.01$, *** $p < 0.001$, **** $p < 0.0001$ *versus* control.

These data supported our results previously acquired from flow cytometry performed with HG reagent, and IC_{25} was thus selected for the following assays.

5.3. Effect of HT on cell viability of hypoxic HK-2 cells

HK-2 cells were exposed to IC_{25} of $CoCl_2$ and/or 5 µM HT for 24 hours at 37°C in 5% CO_2 atmosphere. The MTT reduction assay provided us with results of the effect of IC_{25} of $CoCl_2$ as well as of HT on the viability of the cells, normalized for control. As shown in Figure 17, 5 µM HT solution alone had no notable effect on the viability of the cells (97.6 ± 4.7 % of cell viability). However, although not significantly, HT had a positive effect on the viability of the cells when the cells were exposed to this phenolic compound prior and along with the hypoxia inducer, IC_{25} $CoCl_2$ (77.3 ± 2.8 % of cell viability for the combination of HT + $CoCl_2$ *versus* 75.0 ± 2.0 % of cell viability for $CoCl_2$ alone; $p = 0.280$).

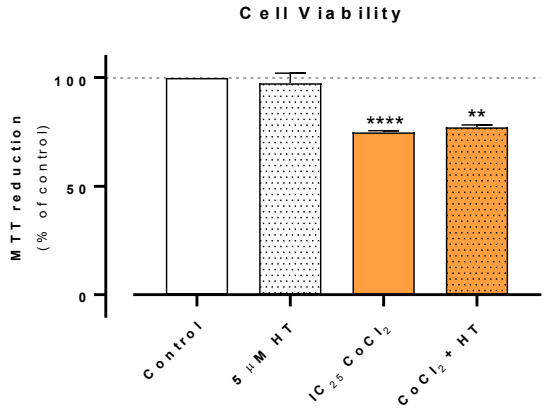

Figure 17 Cell viability of cells exposed to 5 µM HT and/or IC_{25} $CoCl_2$, as determined by the MTT reduction assay. ** $p < 0.01$, **** $p < 0.0001$ *versus* control cells.

5.4. Effect of HT on the oxidative stress status of hypoxic HK-2 cells

HK-2 cells were exposed to IC_{25} of $CoCl_2$ and/or 5 µM HT for 24 hours at 37°C in 5% CO_2 atmosphere. By using a ROS and RNS-sensitive fluorescent probe, we showed that there was a significant increase in the production of reactive species in cells exposed to $CoCl_2$ (Figure 18; 6.0 ± 0.4-fold increase over control, $p < 0.0001$). It also proved that 5 µM HT, though it had no substantial effects on ROS and RNS production over normoxic (control) cells (0.94 ± 0.03-fold increase over control, $p = 0.1480$), had a significant preventive effect on hypoxic cells, i.e. cells exposed to $CoCl_2$ (5.3 ± 0.5-fold increase over control, $p < 0.01$ *versus* $CoCl_2$ alone).

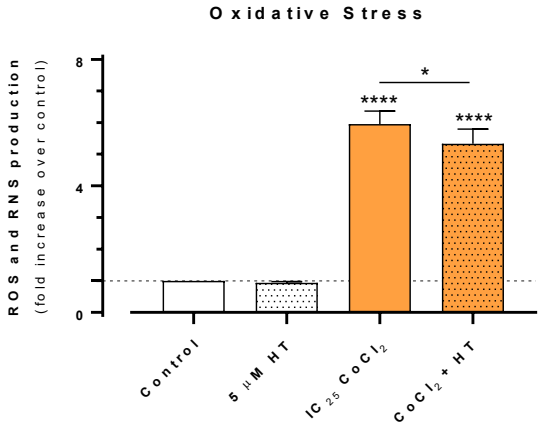

Figure 18 ROS and RNS production, expressed as fold increase over control. * $p < 0.05$; **** $p < 0.0001$ *versus* control.

Furthermore, as shown in Figure 19A, $CoCl_2$ alone elicited a significant depletion of reduced glutathione, the main cellular antioxidant barrier (4.5 ± 1.3 *versus* 8.8 ± 1.8 µmol GSH/mg of protein in control, $p < 0.05$). Though not significantly, HT appeared to prevent this effect of hypoxia on GSH levels (7.6 ± 0.8 µmol GSH/mg of protein for the combination of HT + $CoCl_2$).

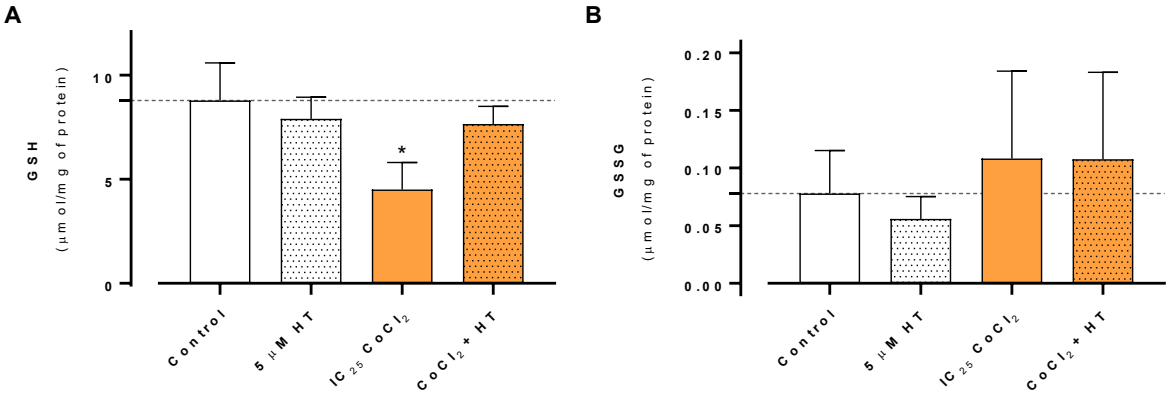

Figure 19 Intracellular levels of (**A**) reduced and (**B**) oxidized glutathione in HK-2 cells exposed to 5 µM HT and/or IC_{25} $CoCl_2$. * $p < 0.05$ *versus* control.

5.5. Effect of HT on the expression of hypoxia-, inflammation-, fibrosis-, and cell death-related genes in hypoxic HK-2 cells

Once we estimated the optimal concentration of $CoCl_2$ to induce hypoxic conditions, we continued to run tests to determine the expression of hypoxia-related genes in cells treated with IC_{25} of $CoCl_2$ and/or 5 µM HT solution. We opted for the same set of hypoxia-related genes as for the evaluation of the best IC of $CoCl_2$ to induce hypoxia: *HIF1A*, *ARNT*, *GAPDH,* and *SPP1*.

As shown in Figure 20, HT appears to have a preventive effect on the hypoxia induced by $CoCl_2$ by reducing the expression of those genes. However, this effect was only significant on the expression of GAPDH, leading to a decrease of mRNA levels of this gene from 7.1 ± 2.6 in cells exposed to $CoCl_2$, to 4.5 ± 1.2 in cells exposed to the combination of HT and the hypoxia inducer ($p < 0.05$).

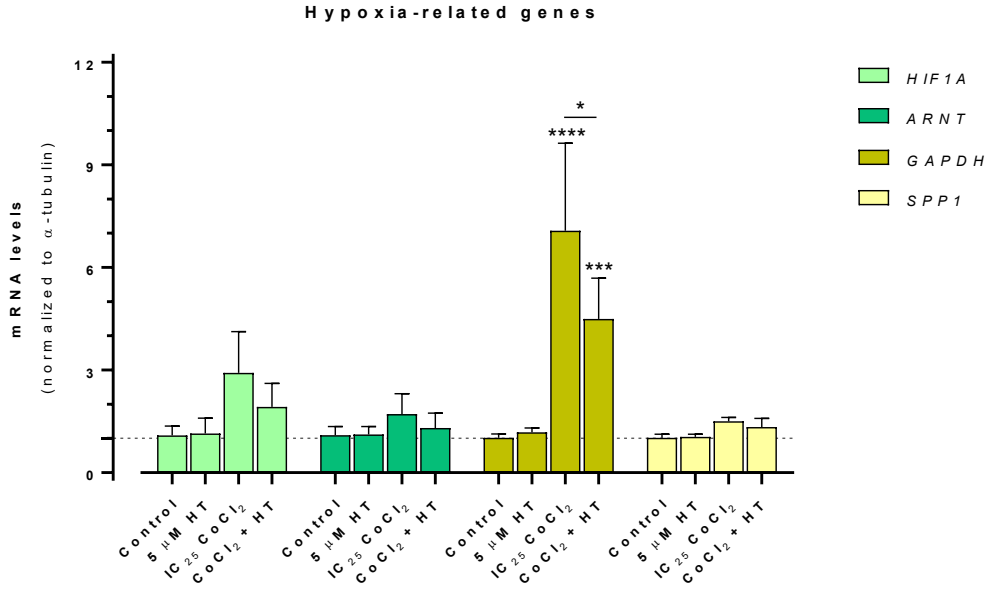

Figure 20 Gene expression of hypoxia-related markers in HK-2 cells exposed to 5 µM HT and/or IC_{25} $CoCl_2$. Data was normalized for the expression of *TUBA1*. * $p < 0.05$; *** $p < 0.001$, **** $p < 0.0001$ *versus* control.

To further understand the mechanisms by which HT affects different processes in hypoxic renal cells, the expression of inflammation-, fibrosis- and cell death-related genes was also determined.

As inflammatory markers, we opted for the evaluation of *IL6* (coding for the cytokine IL-6), *TNF* (coding for the cytokine TNF-α), *NFKB1* (coding for NF-κB), *PTGS2* (coding for the enzyme COX-2) and *CCL2* (coding for the chemokine MCP-1). There was a significant decrease in the mRNA levels of *IL6* from 3.0 ± 1.0 in cells exposed to $CoCl_2$, to 1.1 ± 0.3 in cells exposed to the combination of HT and $CoCl_2$ ($p < 0.0001$), and a slight, but not significant decrease in the expression of *TNF* (from 1.6 ± 0.4 to 1.3 ± 0.3, $p = 0.4705$) and *NFKB1* (from 1.2 ± 0.3 to 0.9 ± 0.4, $p = 0.4213$) in hypoxic conditions when exposed to 5 µM HT (Figure 21). The remaining genes did not seem to be significantly affected by HT.

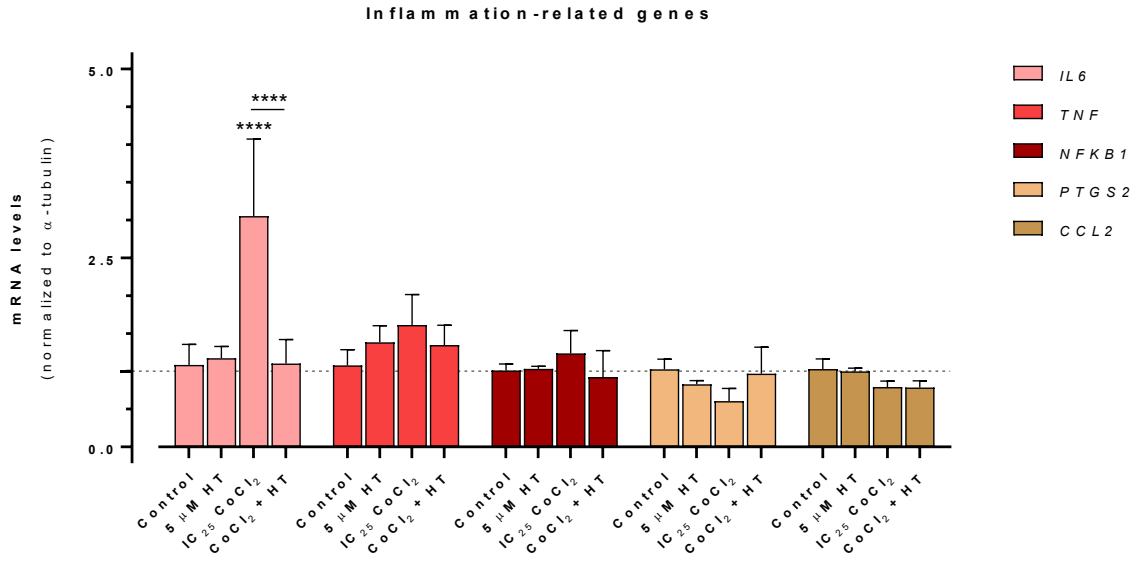

Figure 21 Gene expression of inflammation-related markers in HK-2 cells exposed to 5 µM HT and/or IC_{25} $CoCl_2$. Data was normalized for the expression of *TUBA1*. **** $p < 0.0001$ *versus* control or $CoCl_2$ alone.

For demonstrating the effect of HT on hypoxia-related fibrosis, two fibrosis-related genes were chosen: *TGFB1* (coding for the main fibrotic cytokine TGF-β) and *IL1B* (coding for the pro-inflammatory/pro-fibrotic cytokine IL-1β). The expression of *IL1B* in hypoxic

conditions was not significantly influenced by 5 µM HT (Figure 22). However, we observed a decline in the mRNA levels of this gene from 1.8 ± 0.3 in cells exposed to $CoCl_2$, to 1.2 ± 0.3 in cells exposed to the combination of HT and $CoCl_2$ ($p = 0.1439$). Furthermore, there was a significant decrease in expression of *TGFB1* in hypoxic conditions when exposed to 5 µM HT, with a variation from 1.8 ± 0.3 to 1.1 ± 0.3 ($p < 0.05$).

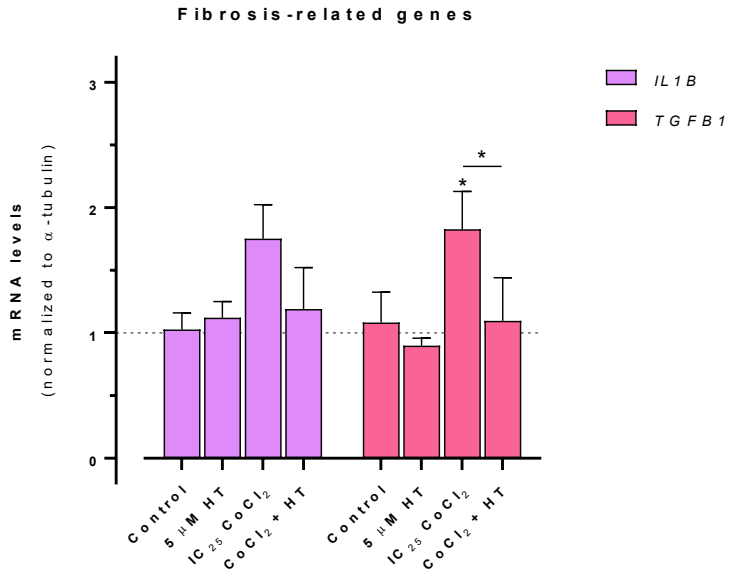

Figure 22 Gene expression of fibrosis-related markers in HK-2 cells exposed to 5 µM HT and/or IC_{25} $CoCl_2$. Data was normalized for the expression of *TUBA1*. * $p < 0.05$ *versus* control or $CoCl_2$ alone.

For the assessment of the involvement of HT on hypoxia-induced renal cell death, we also evaluated the gene expression of *SQSTM1* (encoding for the autophagy-related protein p62), and *CASP3* (encoding for the apoptosis-related protein caspase-3). As demonstrated in Figure 23, induction of renal hypoxia with IC_{25} $CoCl_2$ led to a substantial increase in mRNA levels of *SQSTM1* (4.9 ± 1.2, $p < 0.0001$ *versus* control), but not *CASP3* (1.1 ± 0.0, $p = 0.8124$ *versus* control). Although it appears that HT partially prevented the increased expression of *SQSTM1* on hypoxic conditions (4.1 ± 1.0), this effect was not significant. No effects of HT were observed with regards to *CASP3* expression.

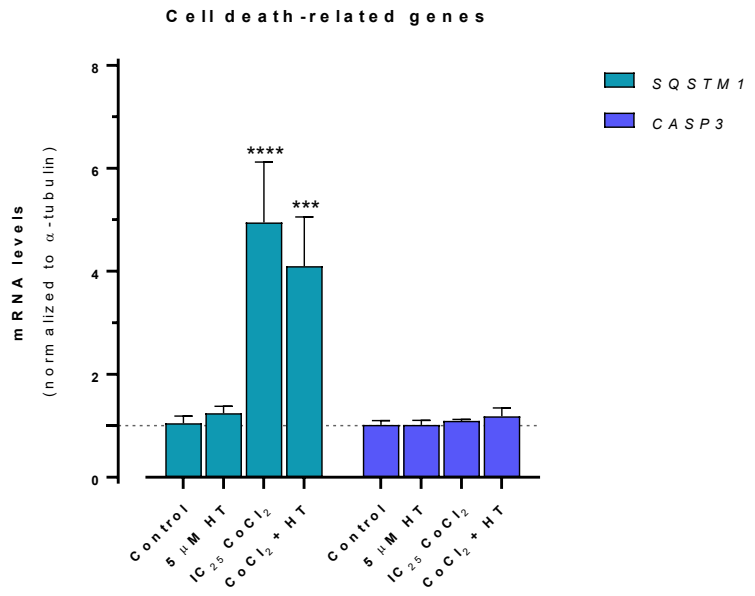

Figure 23 Gene expression of cell death-related markers in HK-2 cells exposed to 5 μM HT and/or IC_{25} $CoCl_2$. Data was normalized for the expression of *TUBA*. *** $p < 0.001$, **** $p < 0.0001$ *versus* control.

5.6. Effects of HT on hypoxia-derived autophagic activation

Considering the observed expression of the autophagic-related gene *SQSTM1* in hypoxic conditions, we further evaluated the formation of AVOs as a marker of autophagic activation through fluorescence microscopy and quantification by flow cytometry. As depicted in Figure 24, the presence of yellow-to-red vesicles is evident in the cytoplasm of HK-2 exposed to IC_{25} $CoCl_2$ (B), which are present at a reduced extent in control cells (A).

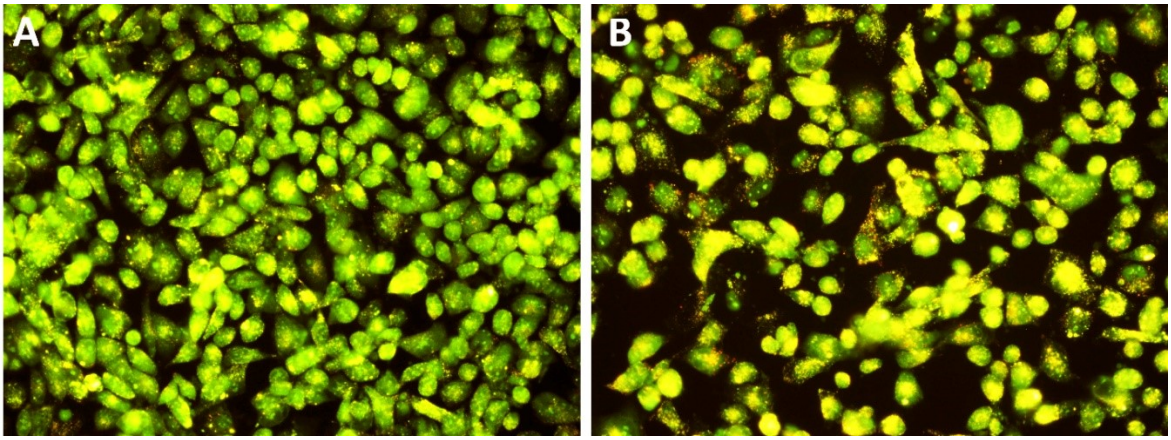

Figure 24 Representative fluorescence micrographs of (A) control cells and (B) HK-2 cells exposed to IC_{25} $CoCl_2$, dyed with acridine orange. Original magnification: 200x.

In order to evaluate the effect of HT on this hypoxia-derived autophagy, AO^+ events were quantified through flow cytometry in cells exposed to 5 µM HT and/or IC_{25} $CoCl_2$. The results are presented in Figure 25. By itself, HT appears to increase the number of AVOs, though not significantly, when compared to control (126.6 ± 7.5 % over control, $p = 0.1241$). In line with the observation of cells under the fluorescence microscope, $CoCl_2$ exposure led to a significant increase in AVOs formation (153.1 ± 7.8 % over control, $p < 0.01$), which was even higher when cells were previously treated with HT (190.9 ± 20.8 % over control, $p < 0.0001$ *versus* control and $p < 0.05$ *versus* $CoCl_2$ alone).

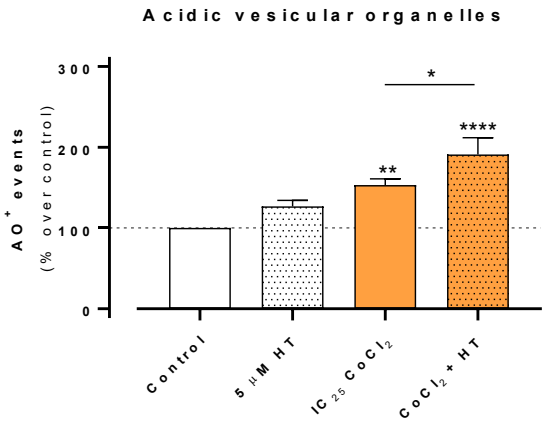

Figure 25 Flow cytometric quantification of AO^+ events in HK-2 cells exposed to 5 µM HT and/or IC_{25} $CoCl_2$. * $p < 0.05$. ** $p < 0.01$, **** $p < 0.0001$ *versus* control.

6. Discussion

Presently, CKD is recognized as a common condition often elevating the risk of CVD, as well as kidney failure. The number of patients with ESRD in need of a kidney transplant or dialysis is on the rise in the recent past and is projected to further increase in the following years. Progression and adverse outcomes can be prevented or postponed through early detection and treatment of CKD. Therefore, it is important to be able to detect earlier stages of CKD through routine laboratory measurements. CKD can be diagnosed without the knowledge of its cause. It is usually determined by markers such as the proteinuria (albumin-creatinine ratio), abnormal urine sediment, or abnormal blood markers. GFR is considered the best measure of overall kidney function. Patients with normal GFR but elevated markers of kidney damage are at increased risk of adverse outcomes of CKD. Because of an age-related decline in GFR, the prevalence of CKD increases with age and requires adjustment in drug dosages in the elderly as well as in other patients with decreased GFR (Levey et al. 2003). The main contributors to the prevalence of CKD remain the diabetes mellitus, hypertension, obesity, cardiovascular disease, or urethral obstruction (Levey et al. 2003; Atkins 2005).

The model of chronic hypoxia and its correlation with impaired kidney function and development of tubulointerstitial fibrosis, as a significant progressive agent in CKD, was generally accepted in the late 1990s (Fine and Norman 2008). The limitation in the oxygen supply of the renal tissue leaves the kidney susceptible to hypoxia and is nowadays considered an important factor in the pathogenesis and progression of CKD. In particular, it induces regulatory mechanisms and gene expression, via HIFs involved in cellular regulation of the glucose metabolism, erythropoiesis angiogenesis, vasotone and cell death/survival decisions (Eckardt et al. 2005). Hypoxia and its close relationship with inflammation have gained general acceptance, based on a study performed in people with mountain sickness, whose levels of pro-inflammatory cytokines (e.g. IL-6, CRP) increased significantly, therefore the development of inflammation in response to hypoxia can be considered clinically relevant. The inflammation can also directly induce hypoxia, as inflamed lesions are prone to, and often become, severely hypoxic. This is due to the increased metabolic and oxygen demands of cells and decrease in metabolic substrates caused by the trauma, compression, thrombosis, or atherosclerosis. Additionally, the multiplication of intracellular pathogens can cause oxygen deprivation of infected cells (Eltzschig and Carmeliet 2011).

As mentioned before, during hypoxia, the amount of HIFs is increased, due to the absence of the rapid ubiquitination and degradation by the 26S proteasome, which happens under normoxic conditions. $CoCl_2$ has been shown to elicit a hypoxic response in several mammalian cells, including normal and tumoral cells (Rana et al. 2019; Tripathi et al. 2019), by inducing the expression of HIF-1α (Muñoz-Sánchez and Chánez-Cárdenas 2018). Accordingly, in HK-2 cells exposed to increasing concentrations of this chemical inducer, we observed an increase in the expression of HIF-1α, in a concentration-dependent manner, up until the IC_{25}. Despite the lack of scienctific evidences regarding a potential effect of $CoCl_2$ on oxygen levels, we also observed a decrease in cellular oxygen levels, as measured by flow cytometry using the HG reagent, which was also dependent on the concentration of the inducer and only significant at IC_{25}. These results require further assays to determine if oxygen deprivation (potentially from decreased production or increased consumption) may actually be an indirect effect of $CoCl_2$.

Although hypoxic conditions have been shown to potentiate the proliferation of tumoral cells from different origins (Vaupel 2014; Sormendi and Wielockx 2018), in the present cell models of normal renal cells, either the HK-2 cell line or the primary cultured HPTECs, the increase in $CoCl_2$ concentration was accompanied by a decrease in cell viability, reaching approximately 100% of cell death at 10 mM $CoCl_2$.

When performing *in vitro* studies, the value of the primary-culture cells obtained from tissue explants is well established, as they may be more representative of the *in vivo* response to a specific stimulus. However, due to the difficulties inherent to the obtention of renal tissue, the laborious and expensive techniques for the isolation and maintenance of purified cells, and the common proliferation limits of primary cultures, immortalized cell lines emerge as convenient alternatives to primary cultures, despite the clear disadvantage of losing some phenotypic and functional characteristics of the original tissue during immortalization procedures (Valente et al. 2011).

In the present study, we showed that HPTECs responded identically to HK-2 cells to $CoCl_2$-induced cell death, as verified by the overlapping concentration-response curves (with a *p*-value > 0.05 for the comparison of the overall curve fits), which supports the use of the immortalized cell line as a suitable alternative to primary cultures to study renal hypoxia.

As shown by the levels of the HG reagent and the expression of hypoxia-related genes, the highest IC of $CoCl_2$ tested (IC_{50}, 491 μM) did not appear to elicit a hypoxic response in HK-2 cells. This is probably due to the inability of cells to react to the hypoxic stimulus when cell death is already extensive, as is the case (50% of cell death, as determined by the MTT reduction assay). Therefore, the selected concentration of $CoCl_2$ to further evaluate the potential beneficial effects of HT in renal hypoxia was the one inducing 25% of inhibition of cell viability (IC_{25}, 254 μM). At this concentration, HT appears to have preventive effects on renal hypoxia, prompting a reduction of *HIF1A* expression when cells are pre-exposed to this phenolic compound prior to the induction of hypoxia. Nevertheless, this preventive effect of HT on renal hypoxia does not appear to translate into prevention of the hypoxia-derived renal damage, as HT had no significant effect on cell death induced by IC_{25} $CoCl_2$, as shown by the MTT reduction assay. Furthermore, the cell death elicited by IC_{25} $CoCl_2$ appears to be independent of the activation of apoptotic cell death, as demonstrated by the absence of variations in the mRNA levels of *CASP3*, which encodes for the apoptosis-related effector caspase 3. In accordance with the MTT reduction data, HT also showed no effect on the expression of this gene under hypoxic conditions. On the other hand, HT appears to contribute for the attenuation of the oxidative stress elicited by the hypoxic response of the HK-2 cells, as shown by a significant decrease of the production of ROS and RNS triggered by $CoCl_2$ in the presence of HT, and the observed reversion of the depletion of reduced glutathione as a major cellular antioxidant defense. In general, the generation of oxygen metabolites under hypoxia rises. The reason behind this might be the close connection between the tissue hypoxia, inflammation and oxidative stress (Ruiz et al. 2013). We can, therefore, state that the observed preventive effects of HT on renal hypoxia are in line with its recognized antioxidant potential (O´Dowd et al. 2004).

HIF-1β subunit is a stable constitutively expressed protein localized in the nucleus, with which the HIF-1α subunit dimerizes under hypoxic conditions, thus enabling their action as transcriptional factors (Ribeiro et al. 2017). As expected, while *HIF1A* expression increased in response to the chemical inducer of hypoxia, the gene encoding for HIF-1β, *ARNT*, did not suffer significant variations up to IC_{25} $CoCl_2$, only diminishing its expression at IC_{50} $CoCl_2$ probably due to the loss of cell integrity observed at this concentration.

OPN is an adhesion molecule, a negatively charged glycosylated phosphoprotein, expressed by the epithelial cells of the kidney, respiratory, and gastrointestinal tract. OPN is involved in several processes, such as the cell signaling, promotion of cell migration, tissue repair, and remodeling, as well as the inhibition of iNOS. According to Sodhi et al. (2000), OPN has both beneficial and harmful effects on the kidney, playing an important role in hypoxia-mediated proliferation in primary cultured glomerular mesangial cells. Beneficial effects of OPN include inhibition of stone formation and renoprotective effect in proximal tubular cells in ischemic injury, whereas the negative effects are connected with increased expression of OPN in various animal models of renal fibrosis, where the increased amount of OPN is associated with a higher influx of monocytes/macrophages (Sodhi, Batlle, and Sahai 2000). In our experiment, we confirmed that the expression of *SPP1*, the gene encoding for the protein OPN, under hypoxic conditions appears to increase dependently of $CoCl_2$ concentration, being significantly higher at IC_{20} and IC_{25} when compared to control cells. On the other hand, the level of *SPP1* expression appears to be slightly decreased when cells are pre-exposed to HT, which further substantiates the beneficial effects of HT on renal hypoxia, and potentially the related renal fibrosis, which may partially rely on the regulation of the expression of this adhesion molecule.

Insufficient intracellular oxygen supply causes upregulating of several transcriptional pathways. Besides HIF itself and OPN expression, the expression of several glycolytic enzymes also increases during hypoxia. GAPDH is one of those glycolytic enzymes, serving for the production of energy. It catalyzes the reversible oxidation of D-glyceraldehyde-3-phosphate to 1,3-diphosphoglycerate. GAPDH also possesses other biological properties, such as the translational regulation, DNA repair and replication, endocytosis, or apoptosis. It is known, that a universal cellular reaction to hypoxia is the induction of expression of glycolytic enzymes, which then cause the shift from oxidative phosphorylation to glycolysis, therefore it is natural for the expression of the GAPDH to be higher in hypoxia-induced cells (Yamaji et al. 2003), as shown by the significant increase in *GAPDH* expression at all ICs of $CoCl_2$ tested. In our experiment, we also found that not only is the expression of *GAPDH* gene higher at hypoxic conditions but that HT acts as an adequate preventive agent in this matter during hypoxia in cells by significantly decreasing its mRNA levels, which further supports the involvement of different hypoxia mediators in the therapeutic effects of HT.

Inflammation has long been recognized as an essential part of CKD. Various inflammatory biomarkers appear to have various predictive values in CKD/ESRD. For example, according to Honda et al. 2006, IL-6 predicts all-cause and cardiovascular mortality better than CRP or other cytokines. The expression of TNF-α and MCP-1 in CKD patients is also elevated (Honda et al. 2006). We examined the impact of hypoxia on the expression of several pro-inflammatory markers and concluded that the expression of pro-inflammatory markers under stress-related stimuli, in our case hypoxia, is indeed increased when compared to the control. HT had a significant preventive effect on the *IL6* expression elicited in the cells exposed to hypoxic conditions, and though not significantly, HT appears to also exert positive effects of the expression of *TNF* and *NFKB1*. To further support the link between inflammation and hypoxia it has been proved that the members of the NF-κB family of transcription factors, which regulate inflammation and arrange immune responses to maintain tissue homeostasis, interact with members of the PHD-HIF pathway. Hypoxia increases the expression and signaling of toll-like receptors, which stimulate leukocyte recruitment, phagocytosis, and adaptive immunity (Eltzschig and Carmeliet 2011). Additionally, inflammatory response in hypoxic injury plays a role in the development of tissue fibrosis. NF-κB, as a primary inflammatory-response mediator, promotes fibrosis in liver, kidney and brain tissue, by acting as a transcriptional regulator for HIF-1α leading to an increase of its expression, which contributes to the inflammatory cell infiltration and cytokines production in the tubulointerstitial area (Liu et al. 2017). Renal fibrosis is a very common pathological indication of progressive CKD, as it is closely connected to renal hypoxia, however, the detailed molecular mechanisms of underlying hypoxia-driven renal fibrosis are still not well decoded. Besides the NF-κB pathway, a TGF-β signaling pathway should be considered when studying this issue. TGF-β, as the most prevalent profibrotic cytokine, plays a key role in progressive renal fibrosis. In fibroblasts, the expression of TGF-β is increased during hypoxia and it is believed that the activation of the TGF-β pathway stimulates myofibroblasts (activated fibroblasts) to produce extracellular matrix proteins. Additionally, there is mounting evidence suggesting that the TGF-β expression and TGF-β-driven epithelial-to-mesenchymal transition is aggravated by the pro-inflammatory cytokine IL-1β in different tissues, including HK-2 cells (Masola et al. 2019; Park et al. 2018; Kolb et al. 2001). The extracellular matrix then deposits in excessive amounts in the interstitium, which leads to the

extension of the distance between the capillaries and nearby nephrons, leading to endothelial dysfunction and peritubular microvascular rarefaction. Furthermore, hypoxia and TGF-β synergistically dysregulate the expression of vascular endothelial growth factor and endothelin, which results in an insufficient angiogenic response and worsening of tubulointerstitial hypoxia (Liu et al. 2017). Considering this interplay between the hypoxia, inflammation and fibrosis, we also evaluated the expression of *IL1B* and *TGFB1* under normoxic and hypoxic conditions, and as expected, we observed an increase in the expression of both genes in cells exposed to IC_{25} $CoCl_2$, though only significant for *TGFB1*, thus supporting the hypoxia-driven inflammatory and fibrotic responses in the kidney. Moreover, HT significantly prevented the expression of *TGFB1* in cells under hypoxia (and not significantly, but substantially, the *IL1B* mRNA levels), which suggest the involvement of this fibrotic signaling pathway in the therapeutic potential of HT.

When observed under the confocal microscope, HK-2 cells under hypoxia showed the evident formation of cytoplasmic vesicles, which instigated the evaluation of a possible autophagic activation triggered by $CoCl_2$. Autophagy is a programmed cellular catabolic mechanism intimately regulated by oxidative stress, functioning as a recycling process that disposes of proteins and organelles that are damaged by oxidative stress (Filomeni, De Zio, and Cecconi 2014). Importantly, studies have shown that hypoxia triggers autophagic activation as a cell survival mechanism, via HIF-1 (Mazure and Pouysségur 2010). Accordingly, we showed that cells exposed to IC_{25} $CoCl_2$ present an increased formation of AVOs, as observed under a fluorescence microscope and quantified by flow cytometry. Additionally, we observed increased mRNA levels of *SQSTM1* under hypoxic conditions, a gene that encodes for p62, a protein involved in the regulation of autophagic activation (Lippai and Lyw 2014).

Recent evidence showes that HT induces autophagic activation as a cell survival mechanism against oxidative stress and inflammation (Cetrullo et al. 2016; De Pablosa et al. 2019). Although HT appears to reduce the mRNA levels of *SQSTM1* in cells under hypoxia, we showed that pre-exposure to HT led to an exacerbation of AVOs formation in HK-2 cells exposed to IC_{25} $CoCl_2$, which supports a role of autophagy regulation in the preventive effects of HT on renal hypoxia. However, further studies are required to confirm this hypothesis.

7. Conclusion

The following conclusions were made from the obtained results:

- HPTECs responded identically to HK-2 cells to $CoCl_2$-induced cell death, presenting similar IC_{50}. In both HK-2 cells and HPTECs, the increase in $CoCl_2$ concentration was accompanied by a decrease in cell viability, reaching approximately 100% of cell death at 10 mM $CoCl_2$.
- Though not significantly, HT appears to induce a slight prevention of hypoxia (IC_{25} $CoCl_2$)-derived renal damage.
- HT appears to contribute to the attenuation of the oxidative stress elicited by the hypoxic response of the HK-2 cells, as it shows a significant decrease in the ROS and RNS production and apparent prevention of GSH depletion triggered by $CoCl_2$.
- The expression of hypoxia-related genes *HIF1A*, *SPP1* and *GAPDH* seems to decrease in the presence of HT, but the only significant decrease was found in the expression of the latter gene.
- The preventive effect of HT on hypoxia-derived inflammation was shown by a significant decrease in the expression of *IL6*, and though not significantly, HT appears to also exert positive effects on the expression of *TNF* and *NFKB1*.
- HT appears to have a preventive effect on the renal fibrosis, as it induces a decrease in the expression of both *IL1B* and *TGFB1*.
- Although HT appears to reduce the expression of *SQSTM1* under hypoxia, we showed that pre-exposure to HT led to an exacerbation of AVOs formation in HK-2 cells exposed to IC_{25} $CoCl_2$, which supports a role of autophagy regulation in the preventive effects of HT on renal hypoxia.

Taken together, our data support the use of HT as a potential therapeutic approach in the treatment of CKD and/or CKD-related clinical features in the future. Nevertheless, further studies are required to validate our hypothesis.

Acknowledgement

I would like to thank Prof. Alice Santos-Silva, Ph.D. and Maria João Valente, Ph.D. for their help with my diploma thesis and their cooperation. I also thank Asst. prof. Iva Boušová, Ph.D. for her support, cooperation and valuable pieces of advice.

8. List of abbreviations

ACT	*O*-acetyl transferase
ADH	alcohol dehydrogenase
AGE	advanced glycation end-product
AKI	acute kidney injury
ALDH	aldehyde dehydrogenase
AO	acridine orange
ARD1	arrest-defective-1
AVOs	acidic vesicular organelles
BSA	bovine serum albumin
cDNA	complementary DNA
CKD	chronic kidney disease
COMT	catechol-*o*-methyl transferase
COX	cyclooxygenase
CRP	C-reactive protein
C-TAD	carboxi-terminal transactivation domain
CVD	cardiovascular disease
dATP	deoxyadenosine triphosphate
DCF	2′,7′-dichlorofluorescein
DCFH	2′,7′-dichlorodihydrofluorescein
DCFH-DA	2′,7′-dichlorodihydrofluorescein diacetate
dCTP	deoxycytidine triphosphate
DF	dilution factor
dGTP	deoxyguanosine triphosphate
DMEM/F12	Dulbecco′s Modified Eagle′s Medium: Nutrient Mixture 12
DMSO	dimethylsulfoxide
DN	diabetic nephropathy
dNTPs	deoxynucleotide triphosphates
DPE	dihydroxyphenylethanol

DTNB	5,5'-dithiobis-(2-nitrobenzoic acid)
dTTP	deoxythymidine triphosphate
EDTA	ethylenediaminetetraacetic acid
eNOS	endothelial nitric oxide synthase
ESRD	end-stage renal disease
FBS	fetal bovine serum
FIH-1	factor inhibiting HIF-1
GAPDH	glyceraldehyde-3-phosphate dehydrogenase
GFR	glomerular filtration rate
GGT	c-glutamyl transferase
GlcA	glucuronic acid
GPx	glutathione peroxidase
GR	glutathione reductase
GSH	glutathione
GSSG	glutathione disulfide
GS-TNB	glutathione-thionitrobenzoic adduct
HG	Hypoxia Green
HIF	hypoxia-inducible factor
HK-2	human kidney-2
HPTECs	human proximal tubular epithelial cells
HREs	hypoxia response elements
HT	3-hydroxytyrosol
HVAlc	homovanillyl alcohol
IC	inhibitory concentration
IL	interleukin
iNOS	inducible nitric oxide synthase
LDL	low-density lipoprotein
MAPK	mitogen-activated protein kinase

MCP-1	monocyte chemoattractant protein 1
mRNA	messenger RNA
MTT	[3-(4,5-dimethylthiazol-2-yl)-2,5-diphenyl tetrazolium] bromide
NADPH	nicotinamid adenine dinucleotide phosphate
NAT	*N*-acetyl transferase
NCDs	non-communicable diseases
NF-κB	nuclear factor kappa B
nNOS	neuronal nitric oxide synthase
NO	nitric oxide
NOS	nitric oxide synthase
N-TAD	amino-terminal transactivation domain
OPN	osteopontin
PBS	phosphate buffered saline
PGE2	prostaglandin E2
PGs	prostaglandins
PHD	prolyl hydroxylase domain
pVHL	von Hippel-Lindau protein
qPCR	quantitative polymerase chain reaction
RAAS	renin-angiotensin-aldosteron system
RBCs	red blood cells
RNS	reactive nitrogen species
ROS	reactive oxygen species
SULT	sulfotransferase
TGF	transforming growth factor
TNB	thionitrobenzoic acid
TNF	tumor necrosis factor
UGT	Uridine 5'-diphospho-glucuronosyl transferase

9. References

Adan, A. , G. Alizada, Y. Kiraz, Y. Baran, and A. Nalbant. 2017. 'Flow cytometry: basic principles and applications', *Critical Reviews in Biotechnology*, 37: 163-76.

Akchurin, O. M., and F. Kaskel. 2015. 'Update on Inflammation in Chronic Kidney Disease', *Blood Purification*, 39: 84-92.

Ariazi, J. L., K. J. Duffy, D. F. Adams, D. Fitch, L. Luo, M. Pappalardi, M. Biju, E. H. DiFilippo, T. Shaw, K. Wiggall, and C. Erickson-Miller. 2017. 'Discovery and Preclinical Characterization of GSK1278863 (daprodustat), A Small Molecule Hypoxia Inducible Factor (HIF)-Prolyl Hydroxylase Inhibitor for Anemia', *The Journal of Pharmacology and Experimental Therapeutics*.

Atkins, R. C. . 2005. 'The epidemiology of chronic kidney disease', *Kidney International*, 67: S14-S18.

Bello, A. K., M. Alrukhaimi, G. E. Ashuntantang, S. Basnet, R. C. Rotter, W. G. Douthat, R. Kazancioglu, A. Kottgen, M. Nangaku, N. R. Powe, S. L. White, D. C. Wheeler, and O. Moe. 2017. 'Complications of chronic kidney disease: current state, knowledge gaps, and strategy for action', *Kidney Int Suppl (2011)*, 7: 122-29.

Bitler, C. M. , T. M. Viale, B. Damaj, and R. Crea. 2005. 'Hydrolyzed Olive Vegetation Water in Mice Has Anti-Inflammatory Activity', *The Journal of Nutrition*, 135: 1475–79.

Brezis, M., and S. Rosen. 1995. 'Hypoxia of the renal medulla - its implications for disease', *The New England Journal of Medicine*, 332: 647-55.

Cetrullo, S., S. D'Adamo, S. Guidotti, R. M. Borzì, and F. Flamigni. 2016. 'Hydroxytyrosol prevents chondrocyte death under oxidative stress by inducing autophagy through sirtuin 1-dependent and -independent mechanisms', *Biochimica et Biophysica Acta*, 1860: 1181–91.

Couser, W. G., G. Remuzzi, S. Mendis, and M. Tonelli. 2011. 'The contribution of chronic kidney disease to the global burden of major noncommunicable diseases', *Kidney International*, 80: 1258-70.

De Pablosa, R. M., A. M. Espinosa-Oliva, R. Hornedo-Ortega, M. Cano, and S. Arguelles. 2019. 'Hydroxytyrosol protects from aging process via AMPK and autophagy; a review of its effects on cancer, metabolic syndrome, osteoporosis, immunemediated and neurodegenerative diseases', *Pharmacological Research*, 143: 58–72.

de Souza, P. A. L. , A. Marcadenti, and V. L. Portal. 2017. 'Effects of Olive Oil Phenolic Compounds on Inflammation in the Prevention and Treatment of Coronary Artery Disease', *nutrients*, 9: 1-22.

Eckardt, K. U., W. M. Bernhardt, A. Weidemann, Ch. Warnecke, Ch. Rosenberger, M. S. Wiesener, and C. William. 2005. 'Role of hypoxia in the pathogenesis of renal disease', *Kidney International*, 68: S46-S51.

Eltzschig, H.K., and P. Carmeliet. 2011. 'Hypoxia and Inflammation', *The New England Journal of Medicine*, 364: 656-65.

Fabiani, R., A. De Bartolomeo, P. Rosignoli, M. Servili, G. F. Montedoro, and G. Morozzi. 2002. 'Cancer chemoprevention by hydroxytyrosol isolated from virgin olive oil through G1 cell cycle arrest and apoptosis', *European Journal of Cancer Prevention*, 11: 351-58.

Fabiani, R., A. De Bartolomeo, P. Rosignoli, M. Servili, R. Selvaggini, G. F. Montedoro, C. Di Saverio, and G. Morozzi. 2006. 'Virgin Olive Oil Phenols Inhibit Proliferation of Human Promyelocytic Leukemia Cells (HL60) by Inducing Apoptosis and Differentiation', *Nutrition and disease*, 136: 614-19.

Feghali, C. A., and T. M. Wright. 1997. 'Cytokines acute and chronic inflammation', *Frontiers in Bioscience 2*: 12-26.

Ferrero-Miliani, L. , O.H. Nielsen, P.S. Andersen, and S.E. Girardin. 2006. 'Chronic inflammation: importance of NOD2 and NALP3 in interleukin-1β generation', *Clinical and Experimental Immunology*, 147: 227-35.

Filomeni, G., D. De Zio, and F. Cecconi. 2014. 'Oxidative stress and autophagy: the clash between damage and metabolic needs', *Cell Death and Differentiation*: 1-12.

Fine, L. G., and J. T. Norman. 2008. 'Chronic hypoxia as a mechanism of progression of chronic kidney diseases: from hypothesis to novel therapeutics', *Kidney International*, 74: 867–72.

Fong, G.H., and K. Takeda. 2008. 'Role and regulation of prolyl hydroxylase domain proteins', *Cell Death and Differentiation*, 15: 635-41.

Fraser, S. D. S., and P. J. Roderick. 2019. 'Kidney disease in the Global Burden of Disease Study 2017', *Nature Reviews Nephrology*, 15: 193-94.

Freedman, S. J., Z. J. Sun, F. Poy, A. L. Kung, D. M. Livingston, G. Wagner, and M. J. Eck. 2002. 'Structural basis for recruitment of CBP/p300 by hypoxia-inducible factor-1α', *PNAS*, 99: 5367-72.

Görlach, A. 2009. 'Regulation of HIF-1α at the Transcriptional Level', *Current Pharmaceutical Design*, 15: 3844-52

Greene, R. J., and N. D. Harris. 2008. *Pathology and Therapeutics for Pharmacists, 3rd edition* (Pharmaceutical Press: London,Chicago).

Hallgrímsson, B., H. Benediktsson, and P. D. Vize. 2003. 'Anatomy and Histology of the Human Urinary System.' in P. Vize, A. S. Woolf and J. Bard (eds.), *The Kidney. From Normal Development to Congenital Disease* (Academic Press).

Han, J., T.P.N. Talorete , P. Yamada, and H. Isoda. 2009. 'Anti-proliferative and apoptotic effects of oleuropein and hydroxytyrosol on human breast cancer MCF-7 cells', *Cytotechnology*, 59: 45-53.

Hon, W.-Ch., M. I. Wilson, K. Harlos, T.D.W. Claridgek, Ch. J. Schofieldk, Ch.W. Pugh, P.H. Maxwell, P.J. Ratcliffe, D.I. Stuart, and E.Y. Jones. 2002. 'Structural basis for the recognition of hydroxyproline in HIF-1a by pVHL', *NATURE*, 417: 975-78.

Honda, H., A.R. Qureshi, O. Heimbürger, P. Barany, K. Wang, R. Pecoits-Filho, P. Stenvinkel, and B. Lindholm. 2006. 'Serum Albumin, C-Reactive Protein, Interleukin 6, and Fetuin A as Predictors of Malnutrition, Cardiovascular Disease, and Mortality in Patients With ESRD', *American Journal of Kidney Diseases*, 47: 139-48.

Jambunathan, N. 2010. 'Determination and Detection of Reactive Oxygen Species (ROS), Lipid Peroxidation, and Electrolyte Leakage in Plants.' in Sunkar R. Plant Stress Tolerance (ed.), *Methods in Molecular Biology (Methods and Protocols)* (Humana Press).

Ke, Q., and M. Costa. 2006. 'Hypoxia-Inducible Factor-1 (HIF-1)', *MOLECULAR PHARMACOLOGY*, 70: 1469-80.

Klahr, S. . 2000. 'Obstructive nephropathy', *Internal medicine*, 39: 355-61.

Koeppen, B.M. , and B.A. Stanton. 2013. *Renal Physiology, 5th edition* (Elsevier).

Kolb, M., P.J. Margetts, D.C. Anthony, F. Pitossi, and J. Gauldie. 2001. 'Transient expression of IL-1β induces acute lung injury and chronic repair leading to pulmonary fibrosis', *The Journal of Clinical Investigation*, 107: 1529-36.

Kruger, N.J. 2002. 'The Bradford Method For Protein Quantitation.' in J.M. Walker (ed.), *The Protein Protocols Handbook, Third Edition* (Humana Press).

Kubista, M. , J.M. Andrade, M. Bengtsson, A. Forootan, J. Jonák, K. Lind, R. Sindelka, R. Sjöback, B. Sjögreen, L. Strömbom, A. Ståhlberg, and N. Zoric. 2006. 'The real-time polymerase chain reaction', *Molecular Aspects of Medicine*, 27: 95–125.

Levey, A. S., and J. Coresh. 2012. 'Chronic kidney disease', *The Lancet*, 379: 165-80.

Levey, A. S., J. Coresh, E. Balk, A. T. Kausz, A. Levin, M. W. Steffes, R. J. Hogg, R. D. Perrone, J. Lau, and G. Eknoyan. 2003. 'National Kidney Foundation Practice Guidelines for Chronic Kidney Disease: Evaluation, Classification, and Stratification', *Annals of internal medicine*, 138: 137-47.

Levey, A. S., K. U. Eckardt, Y. Tsukamoto, A. Levin, J. Coresh, J. Rossert, D. De Zeeuw, T. H. Hostetter, N. Lameire, and G. Eknoyan. 2005. 'Definition and classification of chronic kidney disease: a position statement from Kidney Disease: Improving Global Outcomes (KDIGO)', *Kidney International*, 67: 2089-100.

Levey, A. S., A. C. Schoolwerth, N. R. Burrows, D. E. Williams, K. R. Stith, and W. McClellan. 2009. 'Comprehensive public health strategies for preventing the development, progression, and complications of CKD: Report of an expert panel convened by the Centers for Disease Control and Prevention', *American Journal of Kidney Diseases*, 53: 522-35.

Lippai, M., and P. Lyw. 2014. 'The Role of the Selective Adaptor p62 and Ubiquitin-Like Proteins in Autophagy', *BioMed Research International*: 1-11.

Liu, M., X. Ning, Rong Li, Zhen Yang, Xiaoxia Yang, Shiren Sun, and Qi Qian. 2017. 'Signalling pathways involved in hypoxia-induced renal fibrosis', *Journal of Cellular and Molecular Medicine*, 21: 1248-59.

Loru, D., A. Incani, M. Deiana, G. Corona, A. Atzeri, M. P. Melis, A. Rosa, and M. A. Dessì. 2009. 'Protective effect of hydroxytyrosol and tyrosol against oxidative stress in kidney cells', *Toxicology and Industrial Health*, 25: 301-10.

Manna, C., P. Galletti, V. Cucciolla, G. Montedoro, and V. Zappia. 1999. 'Olive oil hydroxytyrosol protects human erythrocytes against oxidative damages', *The Journal of Nutritional Biochemistry*, 10: 159-65.

Masola, V., A. Carraro, S. Granata, L. Signorini, G. Bellin, P. Violi, A. Lupo, U. Tedeschi, M. Onisto, G. Gambaro, and G. Zaza. 2019. 'In vitro efects of interleukin (IL)-1 beta inhibition on the epithelial-to-mesenchymal transition (EMT) of renal tubular and hepatic stellate cells', *Journal of Translational Medicine*, 17: 1-11.

Mazure, N. M., and J. Pouysségur. 2010. 'Hypoxia-induced autophagy: cell death or cell survival?', *Current Opinion in Cell Biology*, 22: 177-80.

Migliori, M., V. Panichi, M. Fitó, A. Scatena, M. Covas, S. Paoletti, R. De la Torre, A. Bertelli, C. Ronco, and M.-Ch. Dang. 2015. 'Anti-Inflammatory Effect of White Wine in CKD Patients and Healthy Volunteers', *Blood Purification*, 39: 218-23.

Muñoz-Sánchez, J., and M.E. Chánez-Cárdenas. 2018. 'The use of cobalt chloride as a chemical hypoxia model', *Journal of Applied Toxicology*: 1-15.

Netter, F. H. . 2012. *The Netter Collection of Medical Illustrations; Urinary System, Second Edition* (Elsevier).

O´Dowd, Y., F. Driss, P. M.-Ch. Dang, C. Elbim, M.-A. Gougerot-Pocidalo, C. Pasquier, and J. El-Benna. 2004. 'Antioxidant effect of hydroxytyrosol, a polyphenol from olive oil:

scavenging of hydrogen peroxide but not superoxide anion produced by human neutrophils', *Biochemical Pharmacology*, 68: 2003-08.

Park, M.J., S.J. Moon, D.S. Kim, J.H. Lee, and M.L. Cho. 2018. 'IL-1-IL-17 Signaling axis contributes to fibrosis and inflammation in two different murine models of systemic sclerosis', *Frontiers in Immunology*, 9: 1-12.

Rahman, I. , A. Kode, and S. K. Biswas. 2007. 'Assay for quantitative determination of glutathione and glutathione disulfide levels using enzymatic recycling method', *Nature Protocols*, 1: 3159-65.

Rana, N.K., P. Singh, and B. Koch. 2019. '$CoCl_2$ simulated hypoxia induce cell proliferation and alter the expression pattern of hypoxia associated genes involved in angiogenesis and apoptosis', *Biological Research*, 52: 1-13.

Reidy, K., H. M. Kang, T. Hostetter, and K. Susztak. 2014. 'Molecular mechanisms of diabetic kidney disease', *The Journal of Clinical Investigation*, 124: 2333-40.

Ribeiro, S., L. Belo, F. Reis, and A. Santos-Silva. 2017. 'The HIF Response to ESA Therapy in CKD-related Anemia.' in J. Zheng and Ch. Zhou (eds.), *Hypoxia and Human Diseases* (IntechOpen).

Robles-Almazan, M., M. Pulido-Moran, J. Moreno-Fernandez, C. Ramirez-Tortosa, C. Rodriguez-Garcia, J. L. Quiles, and MC. Ramirez-Tortosa. 2018. 'Hydroxytyrosol: Bioavailability, toxicity, and clinical applications', *Food Research International*, 105: 654–67.

Rodríguez-Morató, J., A. Boronat, A. Kotronoulas, M. Pujadas, A. Pastor, E. Olesti, C. Pérez-Mañá, O. Khymenets, M. Fitó, M. Farré, and R. de la Torre. 2016. 'Metabolic disposition and biological significance of simple phenols of dietary origin: hydroxytyrosol and tyrosol', *Drug Metabolism Reviews*, 48: 1-19.

Ruiz, S., P. E. Pergola, R. A. Zager, and N. D. Vaziri. 2013. 'Targeting the transcription factor Nrf2 to ameliorate oxidative stress and inflammation in chronic kidney disease', *Kidney International*, 83: 1029–41.

Ryan, M. J., G. Johnson, Judy Kiiu, Sally M. Fuerstenberg, Richard A. Zager, and Beverly Torok-Storb. 1994. 'HK-2: An immortalized proximal tubule epithelial cell line from normal adult human kidney', *Kidney International*, 45: 48-57.

Santangelo, C., R. Varì, B. Scazzocchio, P. De Sanctis, C. Giovannini, M. D'Archivio, and R. Masella. 2018. 'Anti-inflammatory Activity of Extra Virgin Olive Oil Polyphenols: Which Role in the Prevention and Treatment of Immune-Mediated Inflammatory Diseases?', *Endocrine, Metabolic & Immune Disorders - Drug Targets*, 18: 36-50.

Semenza, G.L. 2002. 'Signal transduction to hypoxia-inducible factor 1', *Biochemical Pharmacology*, 64: 993-98.

Semenza, Gregg L. 2012. 'Hypoxia-inducible factors: mediators of cancer progression and targets for cancer therapy', *Trends in Pharmacological Sciences*, 33: 207-14.

Schrauben, S. J., and J. S. Berns. 2020. 'Hematologic Complications of Chronic Kidney Disease - Anemia and Platelet Disorders.' in P. L. Kimmel and M. E. Rosenberg (eds.), *Chronic renal disease, Second Edition* (Elsevier).

Silverstein, Douglas M. 2009. 'Inflammation in chronic kidney disease: role in the progression of renal and cardiovascular disease', *Pediatric Nephrology*, 24: 1445-52.

Sodhi, Ch.P. , D. Batlle, and A. Sahai. 2000. 'Osteopontin mediates hypoxia-induced proliferation of cultured mesangial cells: Role of PKC and p38 MAPK', *Kidney International*, 58: 691–700.

Sormendi, S., and B. Wielockx. 2018. 'Hypoxia Pathway Proteins As Central Mediators of Metabolism in the Tumor Cells and Their Microenvironment', *Frontiers in Immunology*, 9: 1-19.

Strober, W. . 2015. 'Trypan Blue Exclusion Test of Cell Viability', *Current Protocols in Immunology*, 111: A3.B.1–A3.B.3.

Townsend, R. R. . 2020. 'Pathophysiology of hypertension in chronic kidney disease.' in P. L. Kimmel and M. E. Rosenberg (eds.), *Chronic Renal Disease, Second Edition* (Elsevier).

Tripathi, V.K., S.A. Subramaniyan, and I. Hwang. 2019. 'Molecular and Cellular Response of Co-cultured Cells toward Cobalt Chloride ($CoCl_2$)-Induced Hypoxia', *ACS Omega*, 4: 20882−93.

Valente, M. J., R. Henrique, Vera L. Costa, Carmen Jerónimo, Félix Carvalho, Maria L. Bastos, Paula Guedes de Pinho, and Márcia Carvalho. 2011. 'A Rapid and Simple Procedure for the Establishment of Human Normal and Cancer Renal Primary Cell Cultures from Surgical Specimens', *Establishment of Human Renal Primary Cell Cultures*, 6: 1-8.

Van Meerloo, J., G. J. L. Kaspers, and J. Cloos. 2011. 'Cell Sensitivity Assays: The MTT Assay.' in Ian A. Cree (ed.), *Cancer Cell Culture (Methods and Protocols), Second Edition, Methods in Molecular Biology* (Humana Press).

Vaupel, P. 2014. 'The Role of Hypoxia-Induced Factors in Tumor Progression', *The Oncologist*, 9: 10-17.

Wong, B.W., A. Kuchnio, U. Bruning, and P. Carmeliet. 2013. 'Emerging novel functions of the oxygen-sensing prolyl hydroxylase domain enzymes', *Trends in Biochemical Sciences*, 38: 3-11.

Yamaji, R., K. Fujita, S. Takahashi, H. Yoneda, K. Nagao, W. Masuda, M. Naito, T. Tsuruo, K. Miyatake, H. Inui, and Y. Nakano. 2003. 'Hypoxia up-regulates glyceraldehyde-3-phosphate dehydrogenase in mouse brain capillary endothelial cells: involvement of Na^{+}/Ca^{2+} exchanger', *Biochimica et Biophysica Acta*, 1593: 269–76.

Yaribeygi, H., L. E. Simental-Medía, A. E. Butler, and A. Sahebkar. 2018. 'Protective effects of plant-derived natural products on renal complications', *Journal of Cellular Physiology*: 1-12.

Zámocký, M., B. Gasselhuber, P. G. Furtmüller, and Ch. Obinger. 2012. 'Molecular evolution of hydrogen peroxide degrading enzymes', *Archives of Biochemistry and Biophysics*, 525: 131–44.

Zhang, X., J. Cao, and L. Zhong. 2009. 'Hydroxytyrosol inhibits pro-inflammatory cytokines, iNOS, and COX-2 expression in human monocytic cells', *Naunyn-Schmiedeberg's Archives of Pharmacology*, 379: 581-86.